Supporting information

to

Interplay between Molecular Recognition and Acid-Base Reactivity in Tailored Metal-Based Calix[6]arene Receptors

Martin Lepeintre,[a],[b], Aleksandar Višnjevac,[c] Ivan Jabin[a] and Benoit Colasson*[b]*

[a] Laboratoire de Chimie Organique, Université libre de Bruxelles (ULB), Avenue F.D. Roosevelt 50, CP160/06, B-1050 Brussels, Belgium.

[b] Université Paris Cité, CNRS, Laboratoire de Chimie et de Biochimie Pharmacologiques et Toxicologiques, F-75006 Paris, France.

[c] Physical Chemistry Division, Ruđer Bošković Institute, Bijenička 54, HR-10000 Zagreb, Croatia.

Table of contents

I. Experimental Section

Safety Note. Caution! Although we have not encountered any problems, it should be noted that perchlorate salts of metal complexes with organic ligands are potentially explosive and should be handled only in small quantities with appropriate precautions.

All solvents were reagent grade. ^{1}H NMR spectra were recorded at either 500, 400 or 300 MHz and ^{13}C{1H} NMR spectra were recorded at 100 or 126 MHz. Chemical shifts are expressed in ppm. The following abbreviations were used to describe the spectrum: s (singlet), d (doublet), t (triplet), br (broad). $CDCl_3$ was filtered through a short column of basic alumina to remove traces of DCl. Most of the ^{1}H NMR spectral signals were assigned on the basis of 2D NMR analyses (COSY, HSQC, HMBC). NMR spectra were recorded at 298 K unless otherwise stated. ATR-FTIR spectra were recorded at room temperature. High Resolution ESI-MS were recorded on a ThermoFisher Exactive Orbitrap using methanol as solvent.

Synthesis of [Zn(2)(CH_3CN)](ClO_4)$_2$. To a mixture of ligand **2** (100 mg, 0.0796 mmol) dissolved in a solution acetonitrile (0.5 mL) and chloroform (0.5 mL) was added $Zn(ClO_4)_2.6H_2O$ (29.6 mg, 0.0796 mmol). The solution was then stirred for 1 hour. Diethyl ether (4 mL) was added to the reaction mixture and the resulting white precipitate was collected by centrifugation (5 min, 4000 rpm). The solid residue was dried under vacuum to afford [Zn(**2**)(CH_3CN)](ClO_4)$_2$ as a white powder (105 mg, 0.0689 mmol, 87%). Mp: >230°C. IR: (CH_3CN) ν_{max}: 2980, 2360, 2252, 1442, 1377, 1037, 918. ^{1}H NMR (400 MHz, CD_3CN, 298 K): δ (ppm) 7.40 (s, 3H, Im*H*), 7.32 (s, 6H, Ar*H*), 6.93 (s, 3H, Im*H*), 6.51 (s, 6H, Ar*H*), 5.57 (s, 3H, ArO*H*), 5.23 (s, 6H, CH_2Im), 4.01 (d, J = 14.7 Hz, 6H, ArCH_{ax}), 3.75 (s, 9H, NCH_3), 3.37 (d, J = 14.7 Hz, 6H, ArCH_{eq}), 1.33 (s, 27H, *t*Bu), 0.81 (s, 27H, *t*Bu).^{13}C NMR (126 MHz, CD_3CN, 298 K): δ (ppm) 154.6, 148.9, 148.2, 143.3, 134.1, 133.3, 129.2, 128.5, 127.5, 125.4, 123.9, 65.2, 35.4, 35.0, 34.4, 31.7, 30.7. HRMS (ESI) m/z: [M-2ClO_4^-]$^{2+}$ Calcd for [$C_{81}H_{102}O_6N_6Zn$]$^{2+}$: 659.3571 found: 659.3554.

Synthesis of [Zn(3)(CH_3CN)](ClO_4)$_2$. To a mixture of ligand **3** (100 mg, 0.109 mmol) dissolved in a solution of acetonitrile (0.5 mL) and chloroform (0.5 mL) was added $Zn(ClO_4)_2.6H_2O$ (40.5 mg, 0.109 mmol). The solution was then stirred for 1 hour. Diethyl ether (4 mL) was added to the reaction mixture and the resulting white precipitate was collected by centrifugation (5 min, 4000 rpm). The solid residue was dried under vacuum to afford

[Zn(**3**)(CH_3CN)](ClO_4)$_2$ as a pale orange powder (116 mg, 0.0980 mmol, 90%). Mp: >230°C. IR: (CH_3CN) ν_{max}: 2361, 2341, 1651, 1111. ^{1}H NMR (400 MHz, $CDCl_3$/CD_3CN 1:1, 298 K): δ (ppm) 7.36 (s, 3H, Im*H*), 7.29 (d, *J* = 7.5 Hz, 6H, Ar*H*), 7.20 (t, *J* = 7.5 Hz, 3H, Ar*H*), 6.80 (s, 3H, Im*H*), 6.31 (t, *J* = 7.5 Hz, 3H, Ar*H*), 6.18 (d, *J* = 7.5 Hz, 6H, Ar*H*), 5.92 (s, 3H, ArO*H*), 5.02 (s, 6H, CH_2Im), 3.91 (br, 6H, ArCH_{ax}), 3.62 (s, 9H, NCH_3), 3.43 (d, 6H, ArCH_{eq}).^{13}C NMR (126 MHz, $CDCl_3$/CD_3CN 1:1, 298K) δ (ppm) 157.0, 150.8, 147.3, 133.1, 132.4, 127.8, 126.9, 125.7, 125.3, 125.2, 120.6, 63.9, 34.9, 31.1, 31.1, 30.9. HRMS (ESI): *m/z*: [M-2ClO_4^-]$^{2+}$: Calcd for [$C_{57}H_{54}O_6N_6Zn$]$^{2+}$: 491.1693 found: 491.1691.

II. ^{1}H NMR, ^{13}C NMR, COSY NMR, HSQC NMR, HMBC NMR and complementary NMR experiments for the characterization of [Zn(**2**)(G)](ClO$_4$)$_2$.

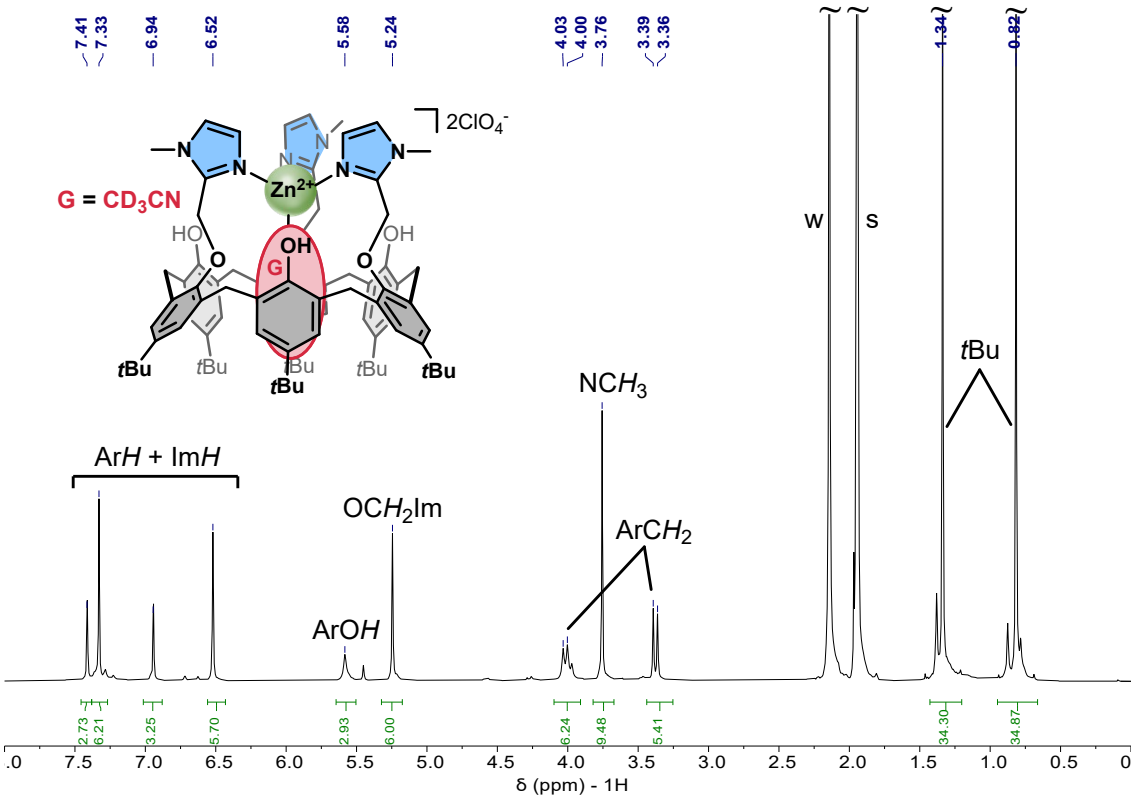

Figure SI1. ^{1}H NMR (298K, 400 MHz) spectrum of [Zn(**2**)(G)](ClO$_4$)$_2$ in CD$_3$CN. S: solvent, w: water.

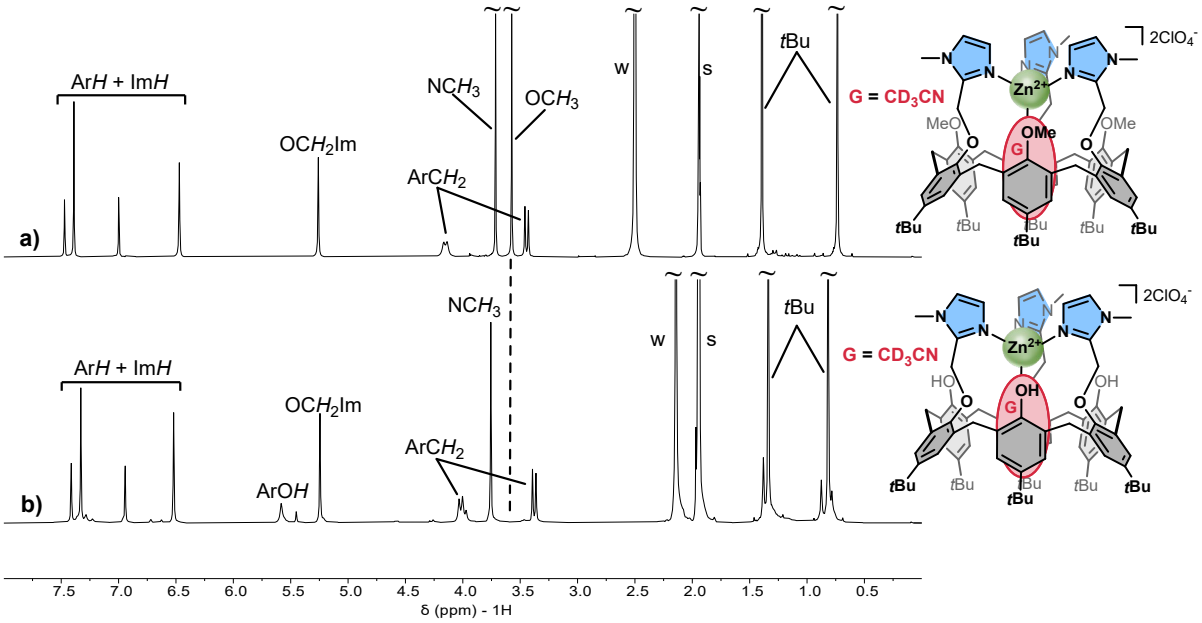

Figure SI2. ^{1}H NMR (298K, a) 400 MHz, b) 500 MHz) spectrum of a) [Zn(**1**)(G)](ClO$_4$)$_2$ in CD$_3$CN and b) [Zn(**2**)(G)](ClO$_4$)$_2$ in CD$_3$CN highlighting the disappearance of the OCH$_3$ resonance at 3.57 ppm.

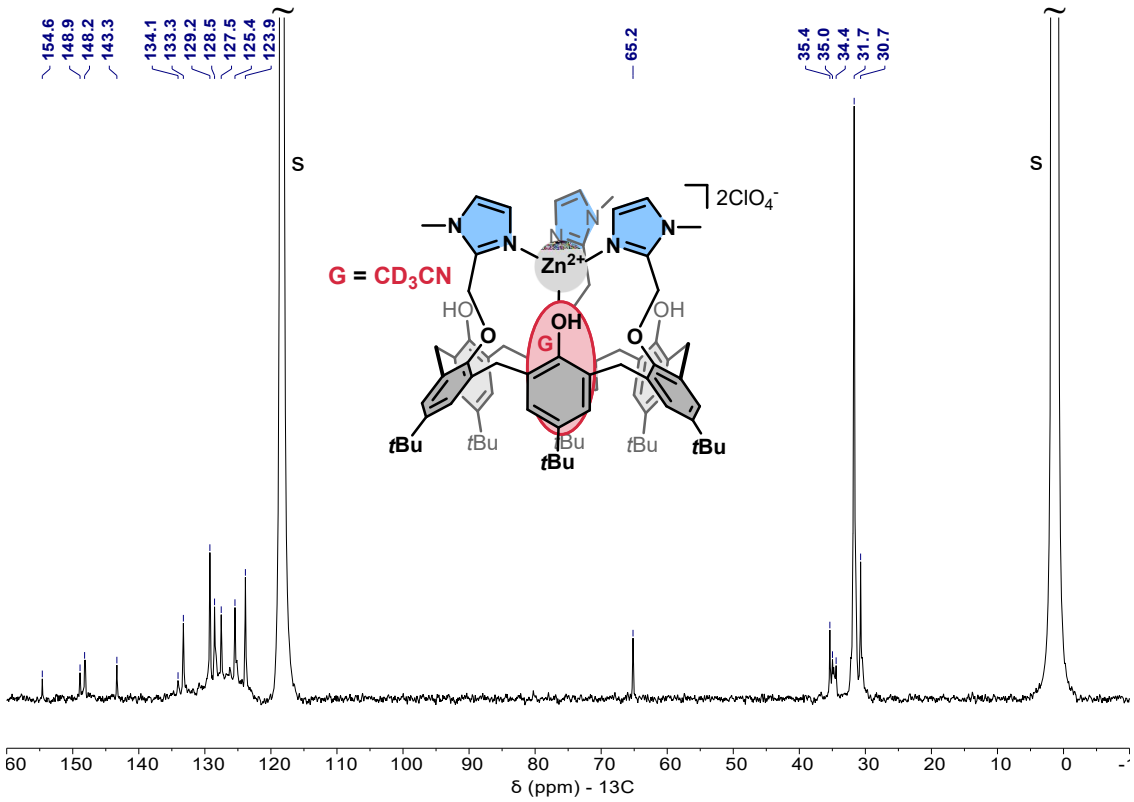

Figure SI3. ^{13}C NMR (298K, 100 MHz) spectrum of [Zn(**2**)(G)](ClO$_4$)$_2$ in CD$_3$CN. S: solvent.

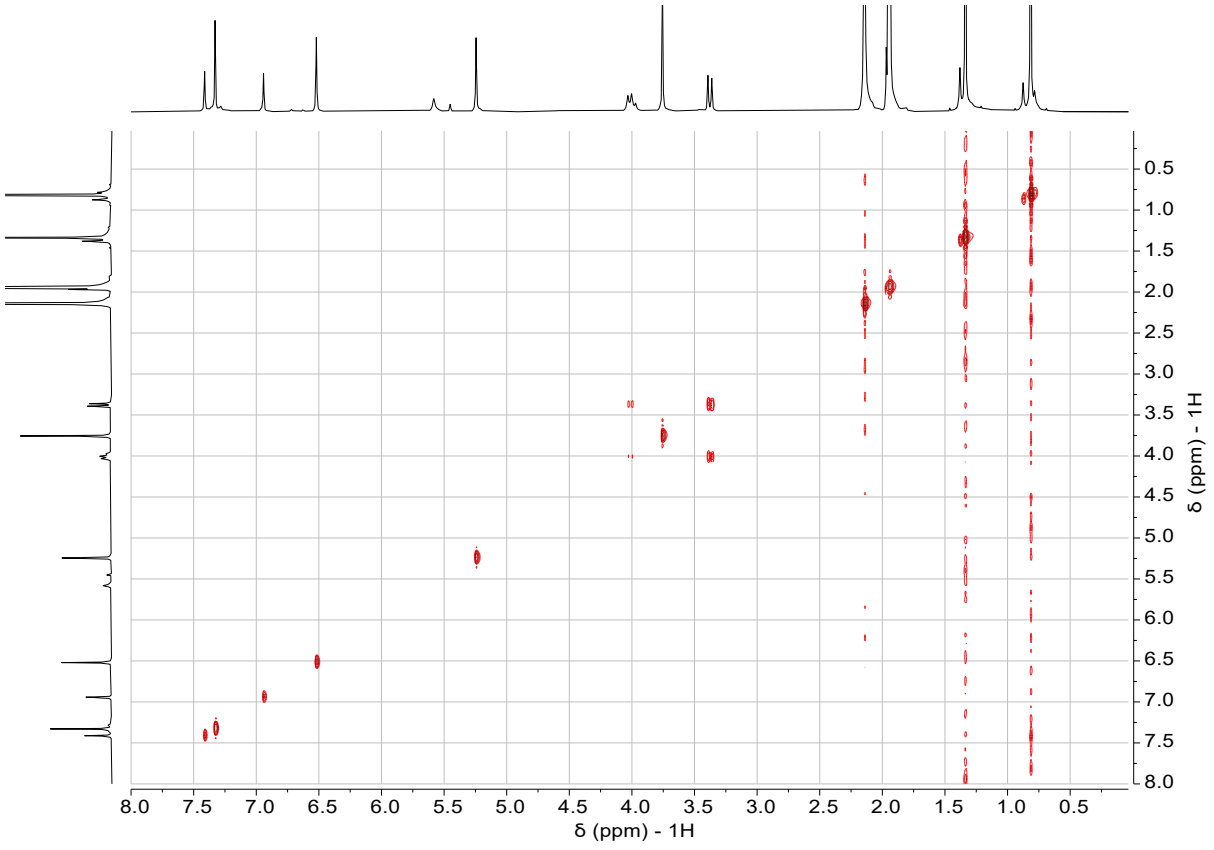

Figure SI4. COSY NMR (298K, 400 MHz) spectrum of [Zn(**2**)(G)](ClO$_4$)$_2$ in CD$_3$CN.

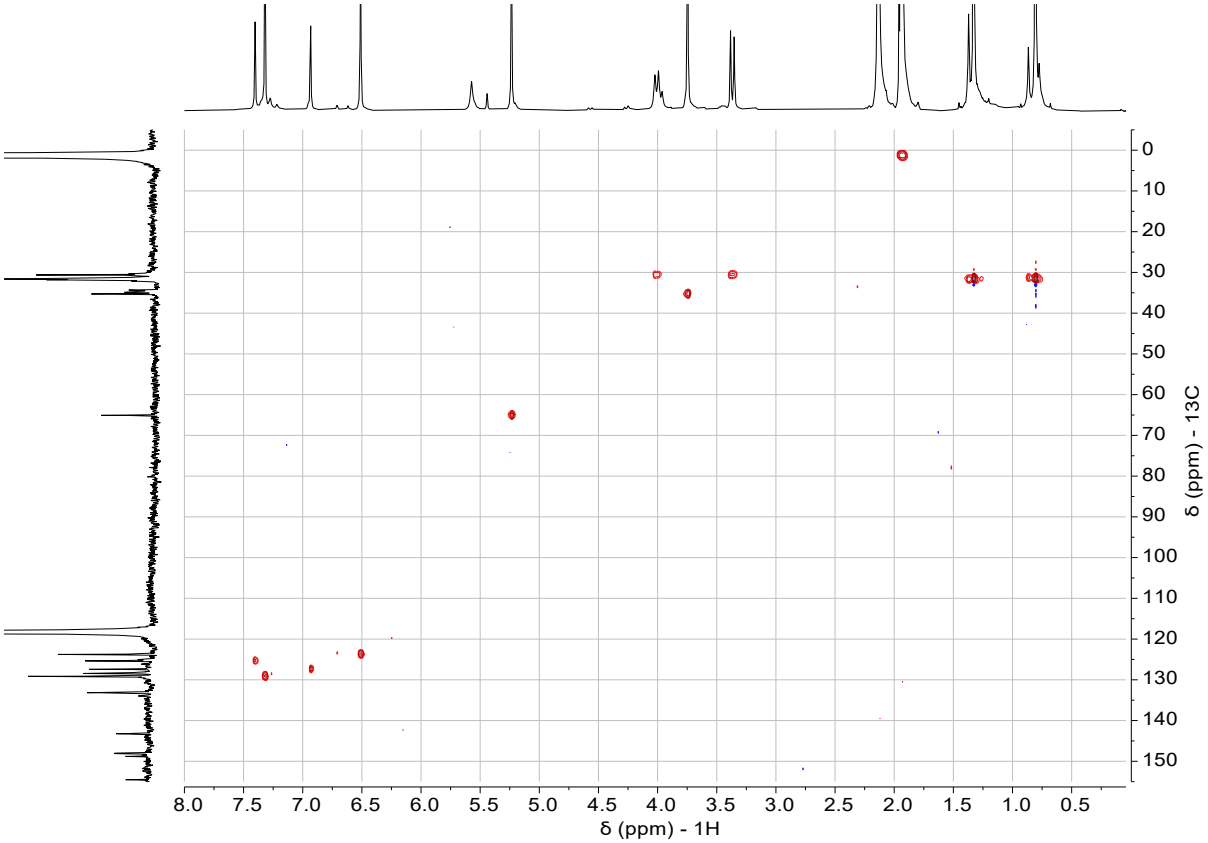

Figure SI5. HSQC NMR (298K, 400 MHz) spectrum of [Zn(**2**)(G)]$(ClO_4)_2$ in CD_3CN.

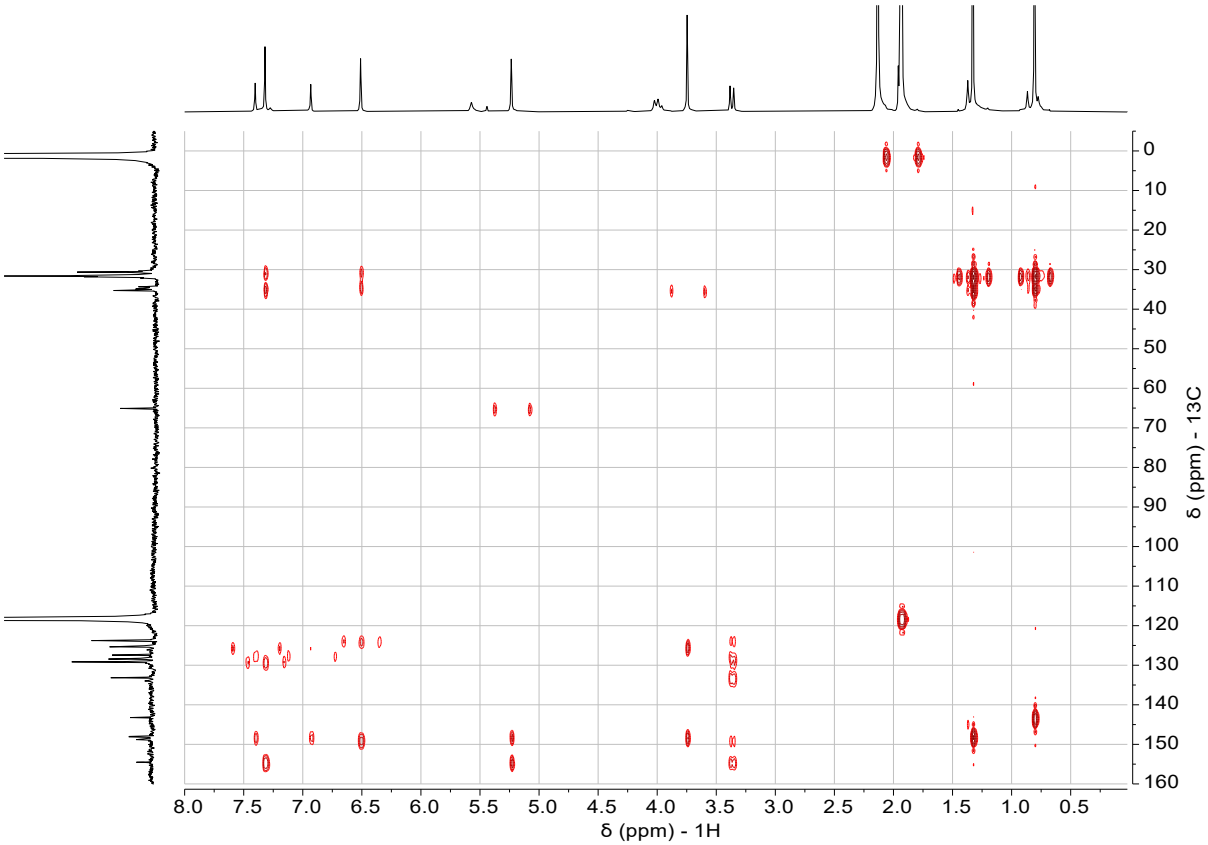

Figure SI6. HMBC NMR (298K, 400 MHz) spectrum of [Zn(**2**)(G)]$(ClO_4)_2$ in CD_3CN.

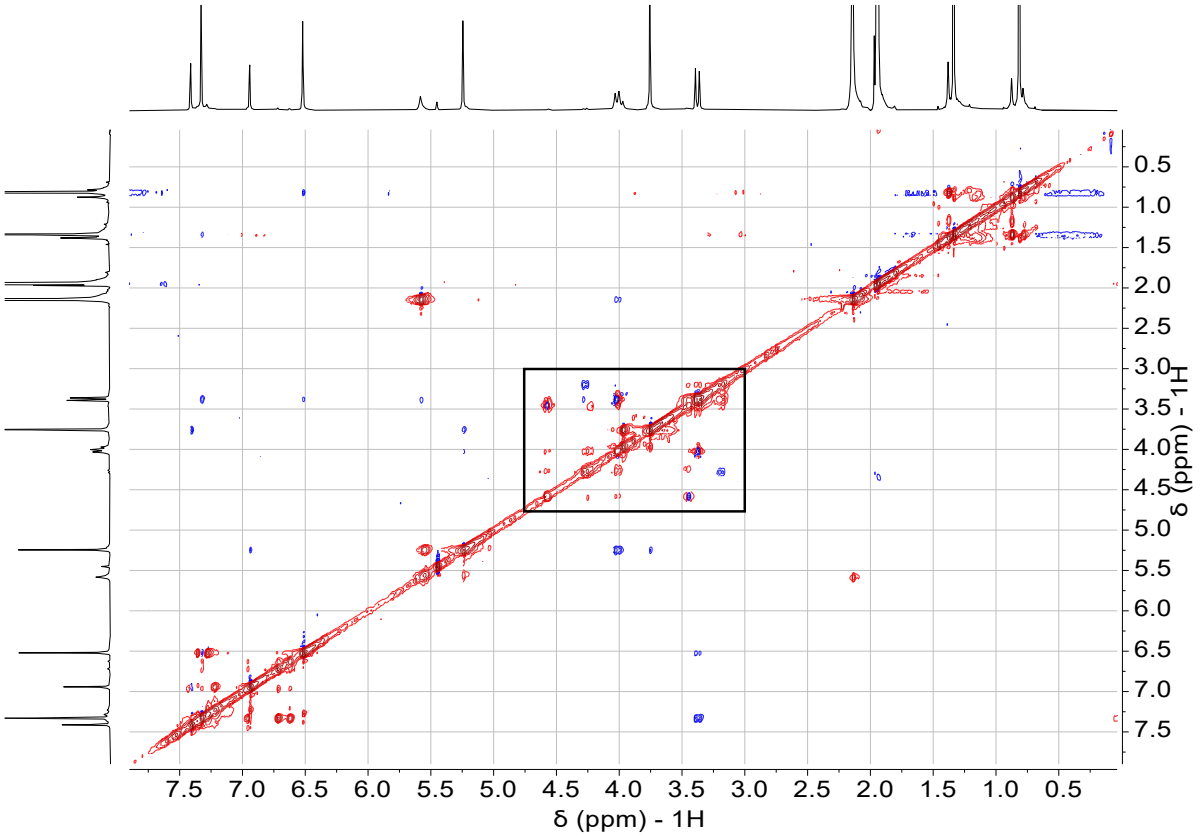

Figure SI7. ROESY NMR (298K, 400 MHz) spectrum of $[Zn(\mathbf{2})(G)](ClO_4)_2$ in CD_3CN.

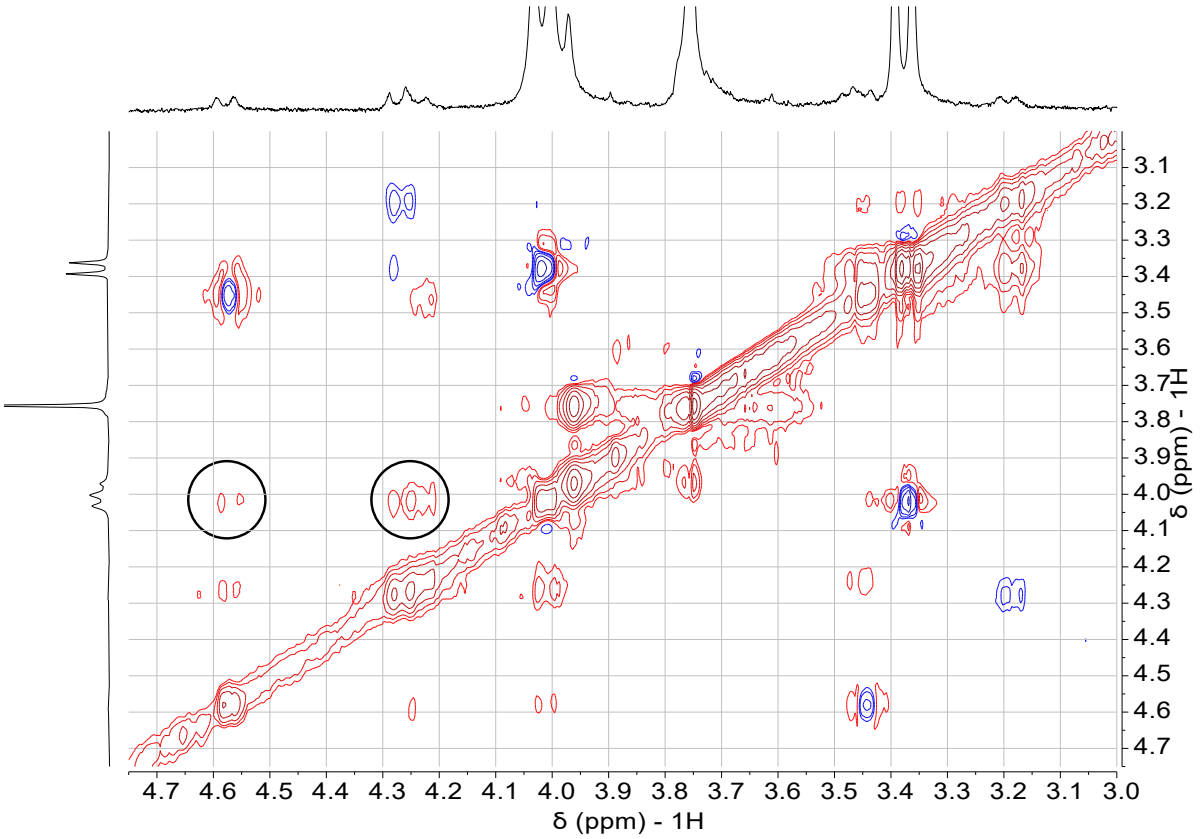

Figure SI8. ROESY NMR (298K, 400 MHz) spectrum of $[Zn(\mathbf{2})(G)](ClO_4)_2$ in CD_3CN, zoomed in on the zone of interest, showing exchange correlations between the minor species and the major species.

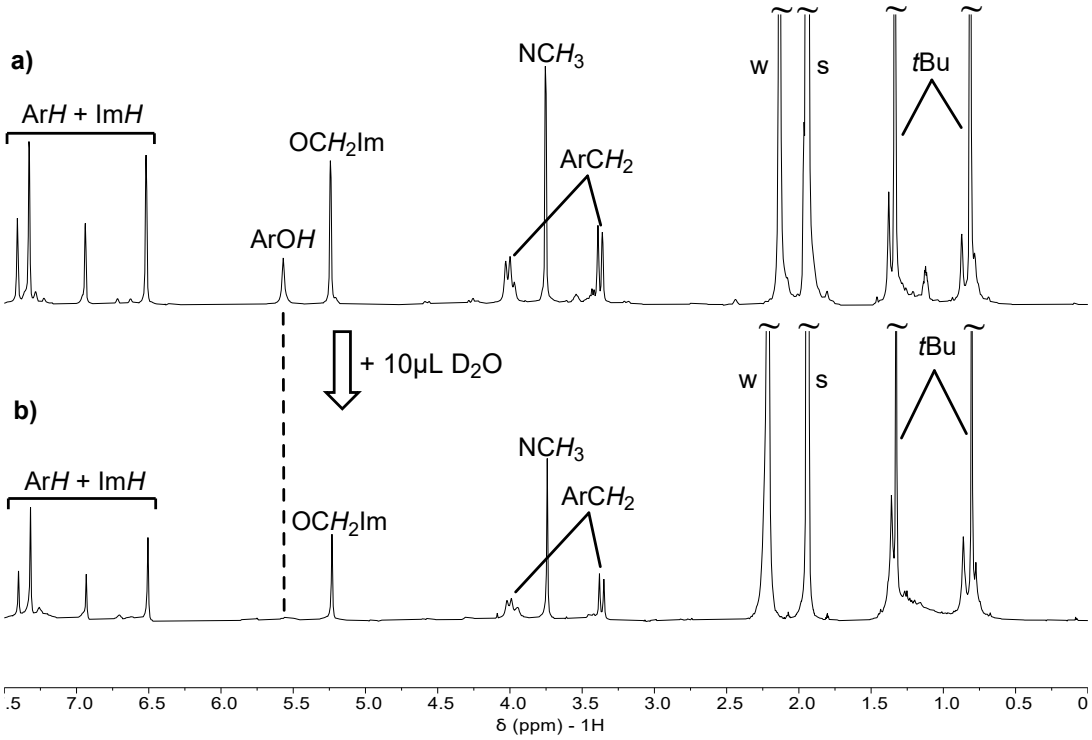

Figure SI9. ^{1}H NMR (298K, 400 MHz) spectrum of [Zn(**2**)(G)]$(ClO_4)_2$ in CD_3CN with addition of D_2O in order to identify labile protons of the ArOH units (5.58 ppm): a) before addition and b) after addition of 10µl of D_2O. S: solvent, w: water.

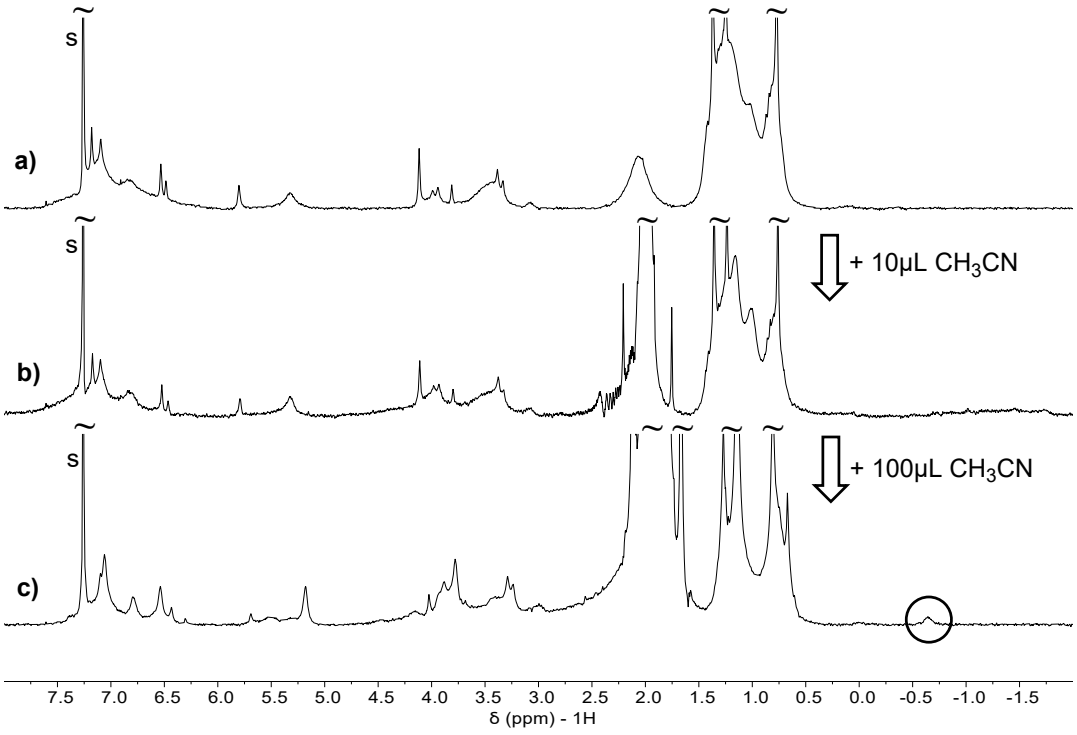

Figure SI10. ^{1}H NMR (298K, 300 MHz) spectrum of [Zn(**2**)(G)]$(ClO_4)_2$ in $CDCl_3$ with addition of CH_3CN to observe the chemical shift of the CH_3 of the acetonitrile guest included inside the cavity: a) before addition, b) after addition of 10µl of CH_3CN and c) after addition of 100µl of CH_3CN. S: solvent. Additional note: The complex was not fully soluble in chloroform, however, the experiment was conducted in chloroform as no signs of inclusion were observed when CD_3CN or a 1:1 mixture of $CD_3CN/CDCl_3$ were used.

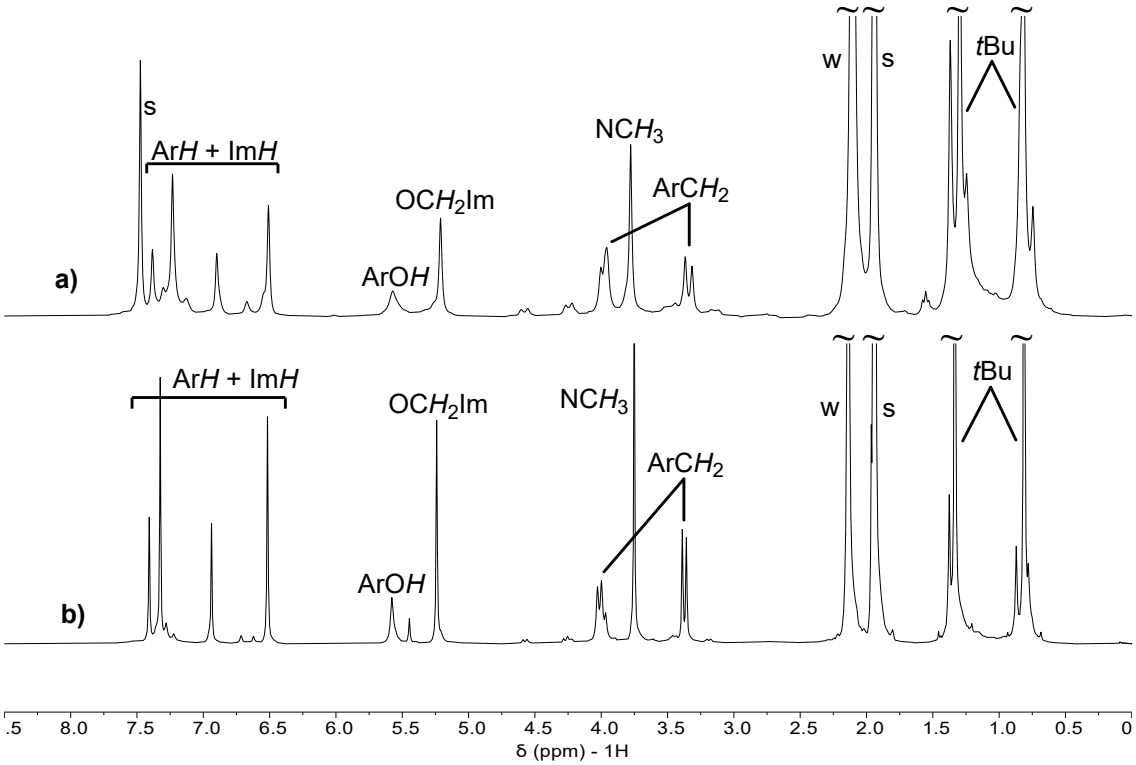

Figure SI11. ^{1}H NMR (298K, 400 MHz) spectrum of [Zn(**2**)(G)]$(ClO_4)_2$ in a) $CDCl_3/CD_3CN$ 1:1 and b) CD_3CN. Additional note: [Zn(**2**)(G)]$(ClO_4)_2$ in CD_3CN exhibited sharper peaks than in a 1:1 $CDCl_3/CD_3CN$ mixture, so characterization was performed in CD_3CN. For titrations, a 1:1 $CDCl_3/CD_3CN$ mixture was used for solubility reasons.

III. ^{1}H NMR, ^{13}C NMR, COSY NMR, HSQC NMR, HMBC NMR and complementary NMR experiments for the characterization of [Zn(**3**)(G)]$(ClO_4)_2$.

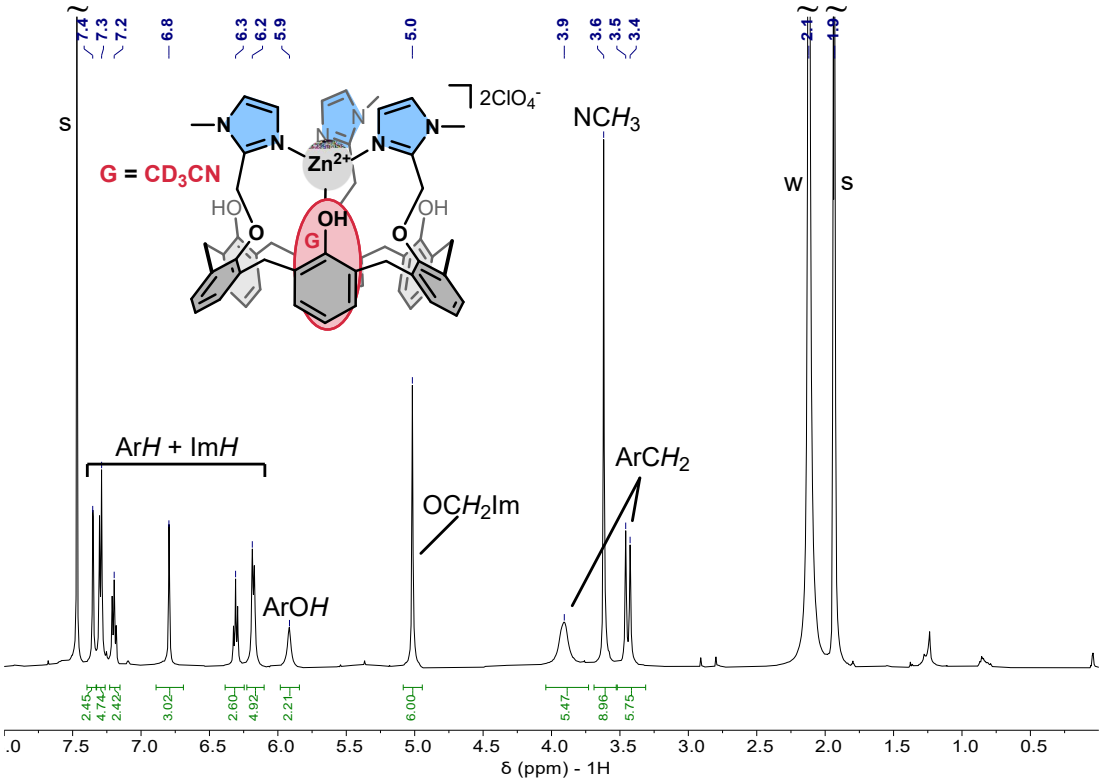

Figure SI12. ^{1}H NMR (298K, 400 MHz) spectrum of [Zn(**3**)(G)]$(ClO_4)_2$ in $CD_3CN/CDCl_3$ 1:1. S: solvent, w: water.

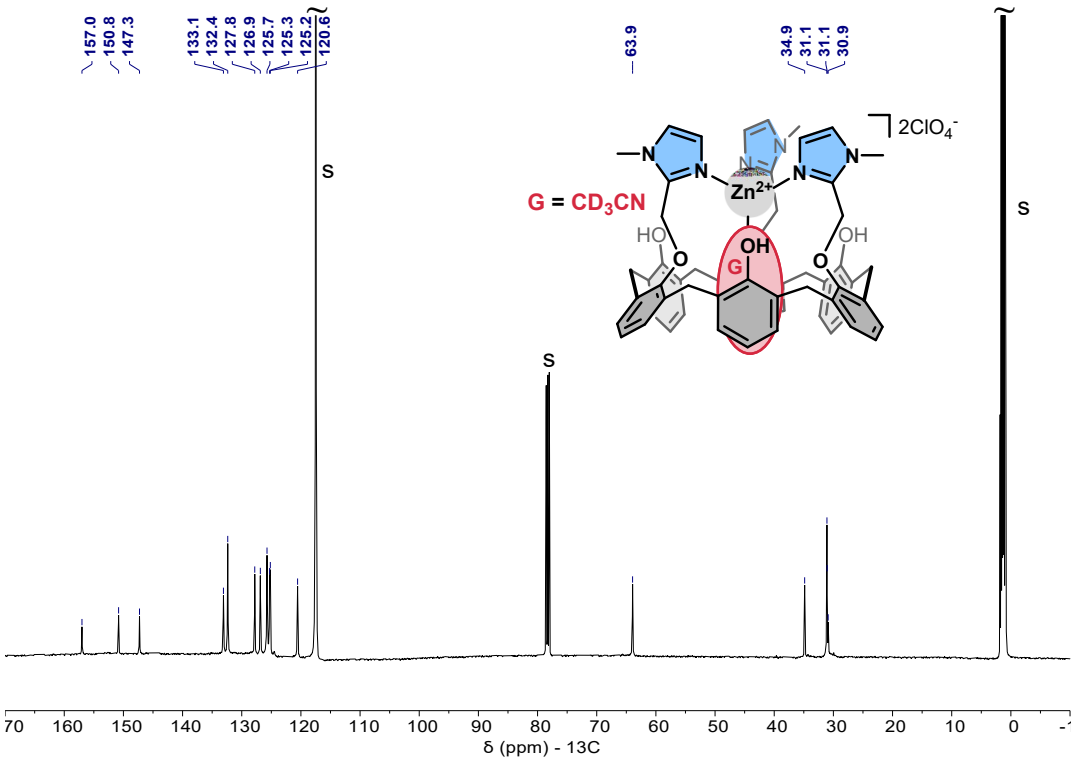

Figure SI13. ^{13}C NMR (298K, 100 MHz) spectrum of [Zn(**3**)(G)]$(ClO_4)_2$ in $CD_3CN/CDCl_3$ 1:1. S: solvent.

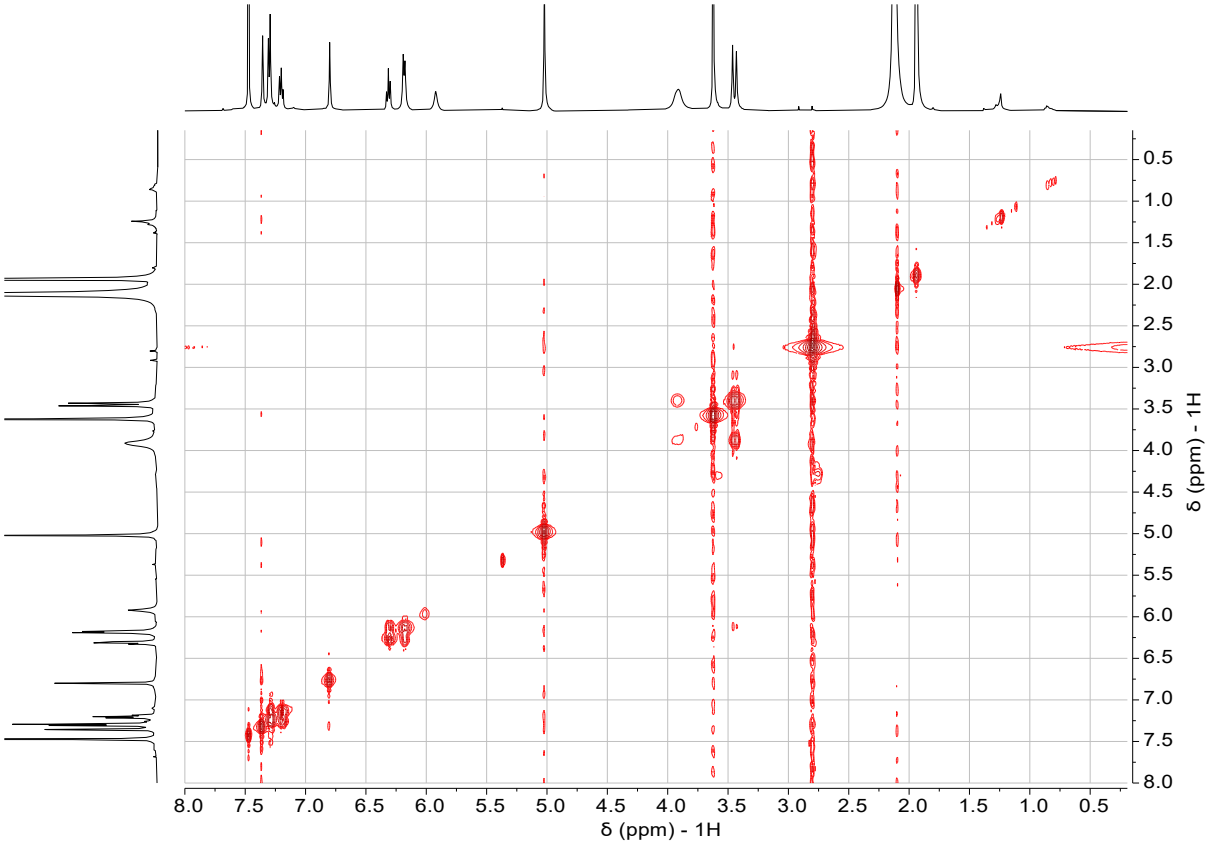

Figure SI14. COSY NMR (298K, 400 MHz) spectrum of [Zn(**3**)(G)]$(ClO_4)_2$ in $CD_3CN/CDCl_3$ 1:1.

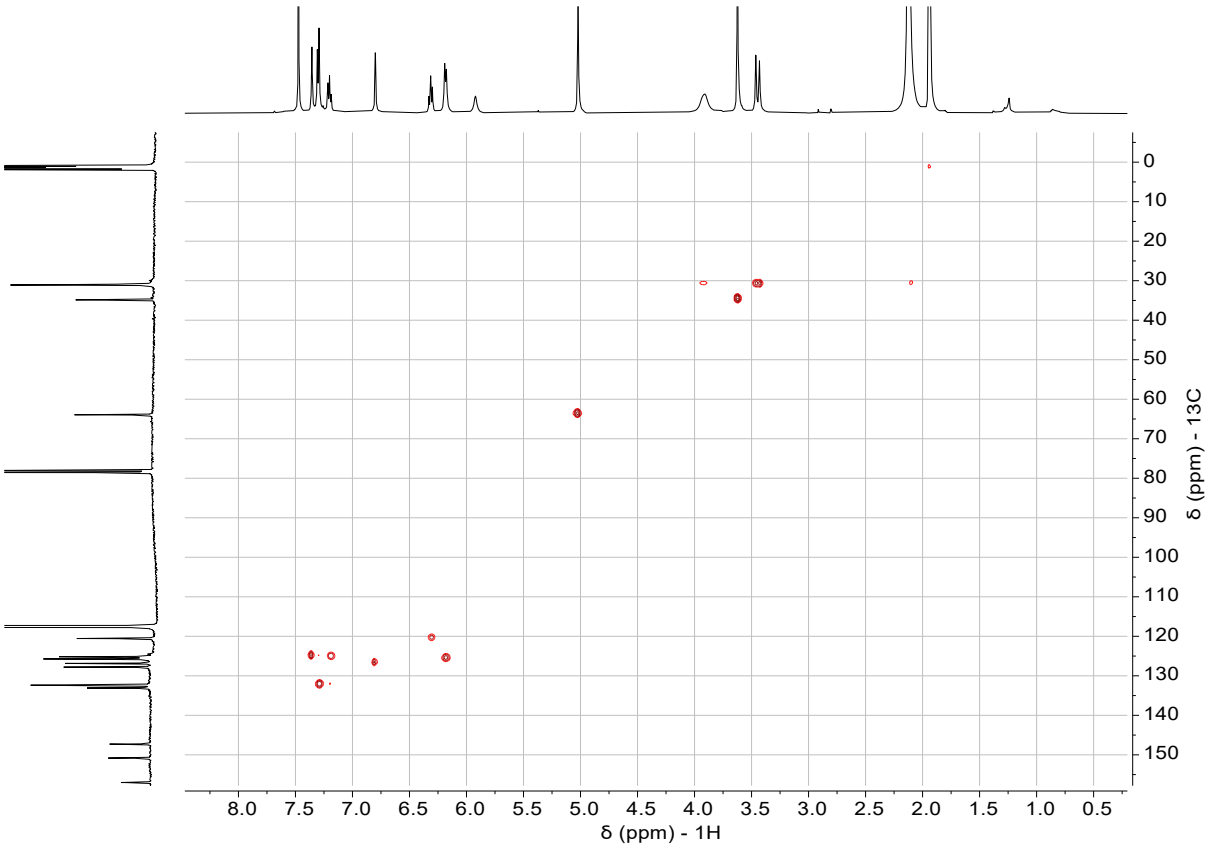

Figure SI15. HSQC NMR (298K, 400 MHz) spectrum of [Zn(**3**)(G)]$(ClO_4)_2$ in $CD_3CN/CDCl_3$ 1:1.

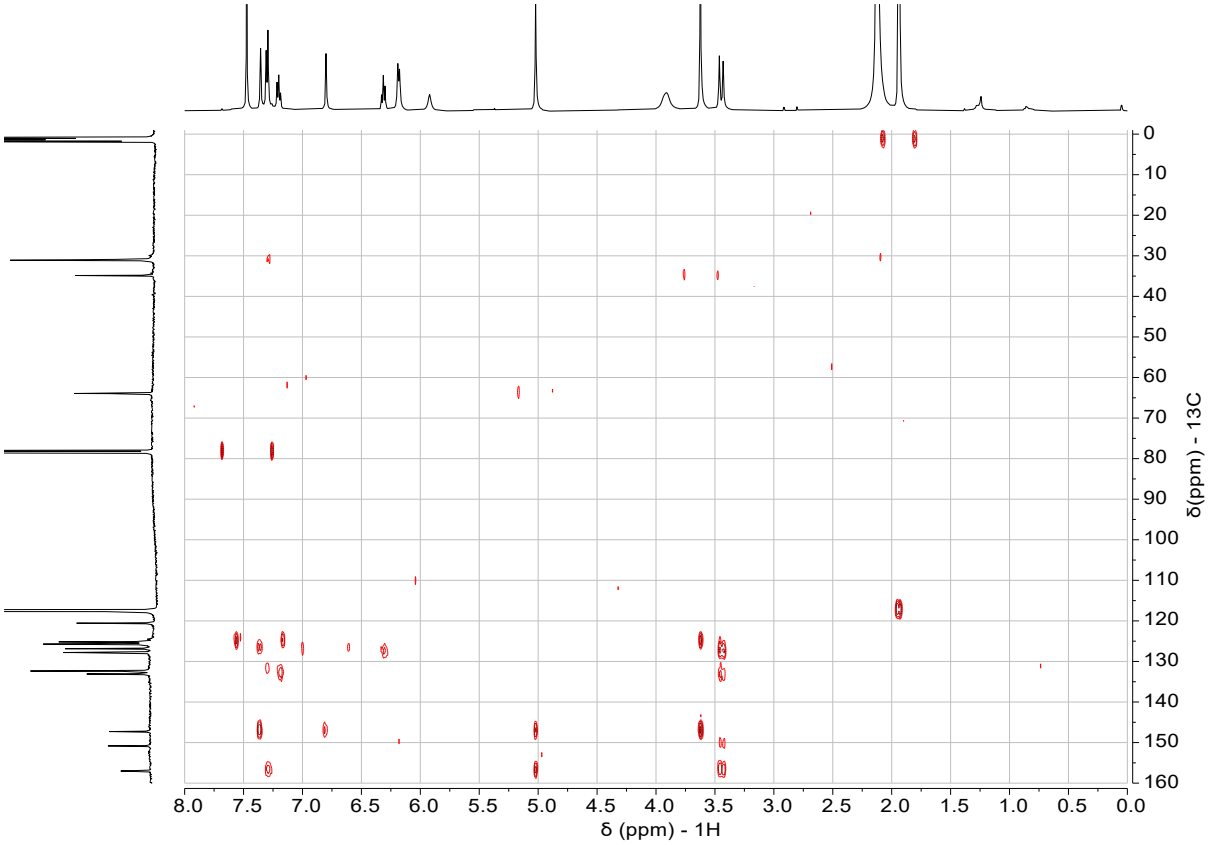

Figure SI16. HMBC NMR (298K, 400 MHz) spectrum of $[Zn(\mathbf{3})(G)](ClO_4)_2$ in $CD_3CN/CDCl_3$ 1:1.

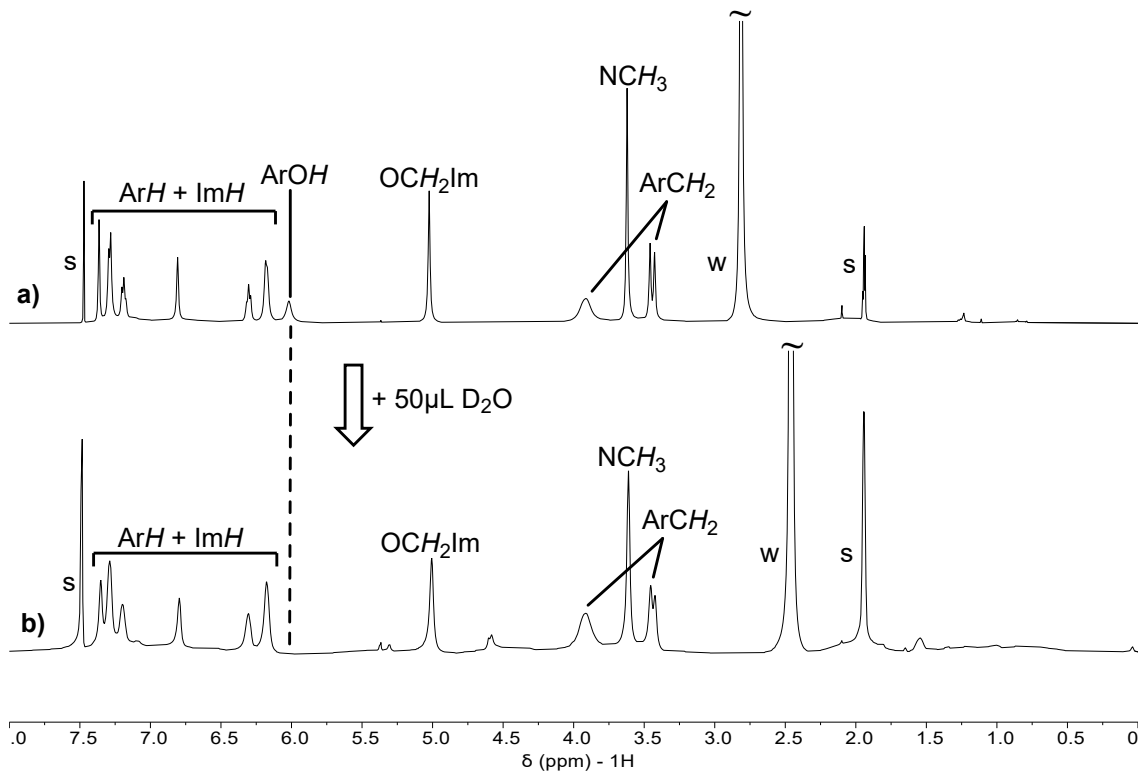

Figure SI17. ^{1}H NMR (298K, 400 MHz) spectrum of $[Zn(\mathbf{3})(G)](ClO_4)_2$ in CD_3CN with addition of D_2O in order to identify labile protons: a) before addition and b) after addition of 50µl of D_2O. S: solvent, w: water. Additional note: The water peak in spectrum a) is shifted due to the excess zinc salt added to form the zinc complex in situ.

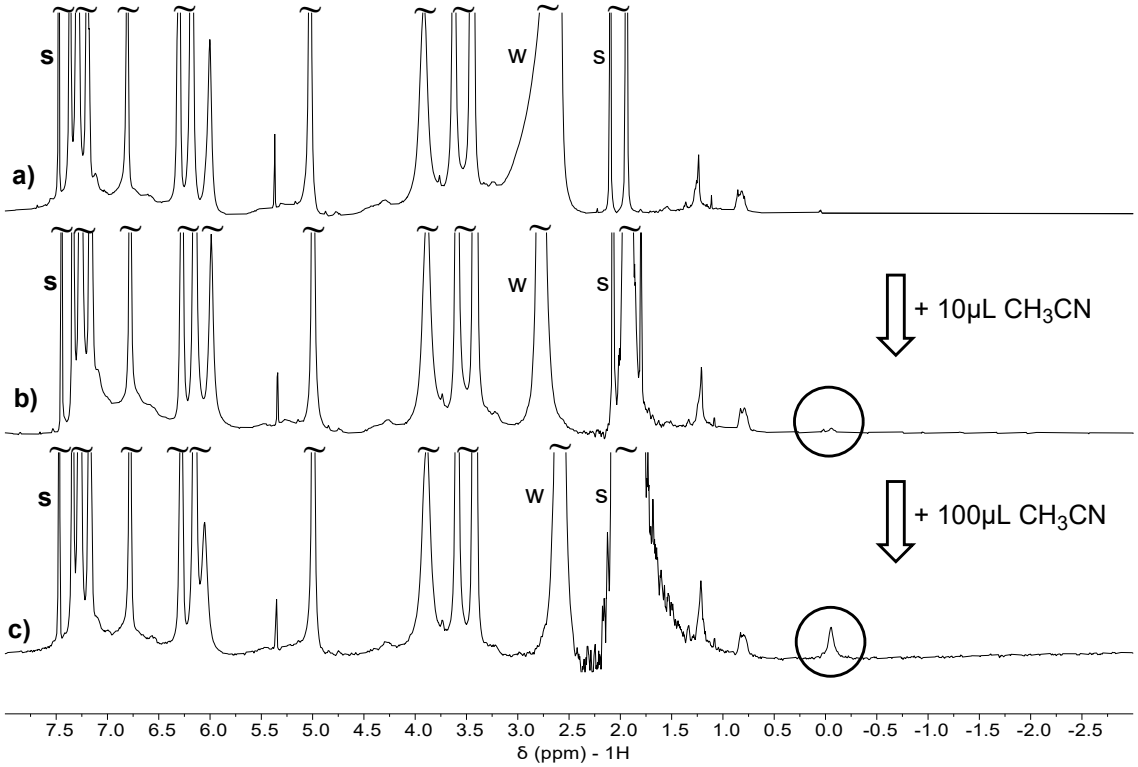

Figure SI18. ^{1}H NMR (298K, 400 MHz) spectrum of [Zn(**3**)(G)]$(ClO_4)_2$ in $CDCl_3/CD_3CN$ with addition of CH_3CN to observe the chemical shift of the CH_3 of the acetonitrile guest included inside the cavity: a) before additions, b) after addition of 10µl of CH_3CN and c) after addition of 100µl of CH_3CN. S: solvent. w: water.

IV. ^{1}H NMR, ^{13}C NMR, COSY NMR, HSQC NMR and HMBC NMR spectra [Zn(**2**)(G)]$(ClO_4)_2$ in $CD_3CN/CDCl_3$ 1:1 with addition of propylamine.^{1}H NMR of [Zn(**2**)(G)]$(ClO_4)_2$ calix[6]arene in $CD_3CN/CDCl_3$ 1:1 with addition of DBU (1,8-Diazabicyclo[5.4.0]undec-7-ene) and comparison to [Zn(**2**)(G)]$(ClO_4)_2$ with addition of propylamine. ^{1}H NMR of **2** in $CD_3CN/CDCl_3$ 1:1 with addition of DBU (1,8-Diazabicyclo[5.4.0]undec-7-ene).

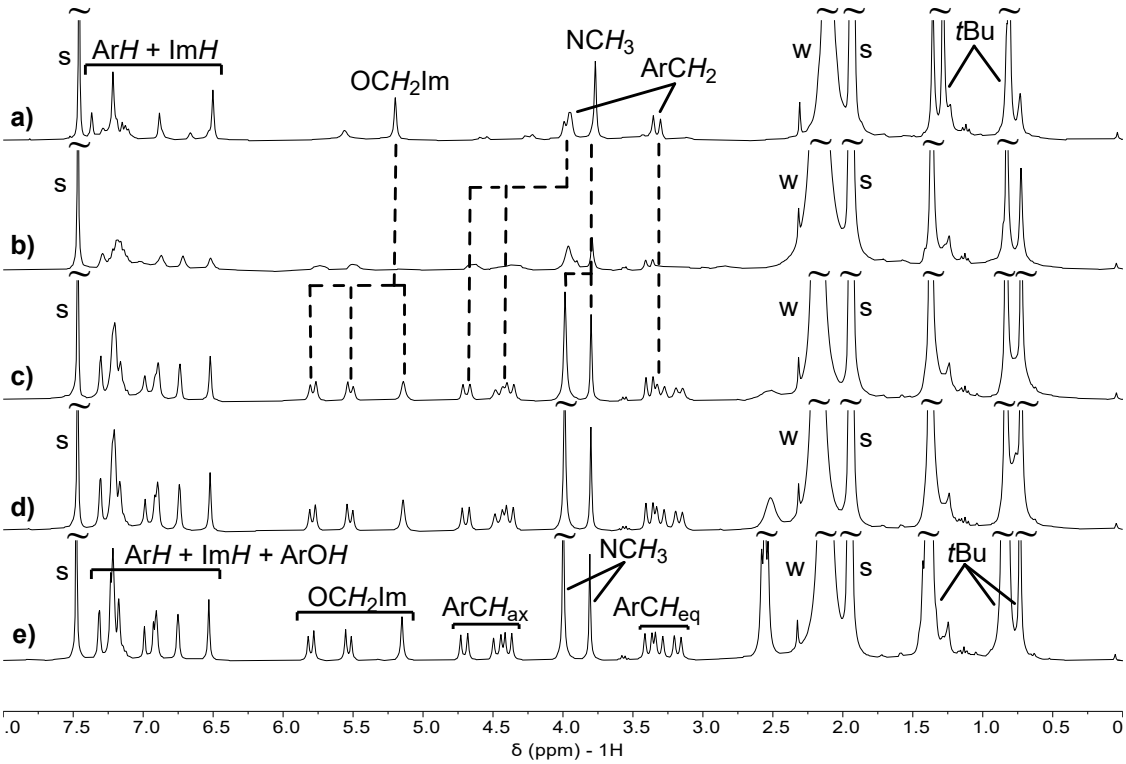

Figure SI19. ^{1}H NMR (298K, 400 MHz) titration showing the evolution of [Zn(**2**)(G)]$(ClO_4)_2$ in $CDCl_3/CD_3CN$ 1:1 v:v during the addition of a) before additions, b) 1 equiv. of propylamine, c) 2 equiv. of propylamine, d) 3 equiv. of propylamine and e) 8 equiv. of propylamine. S: solvent, w: water.

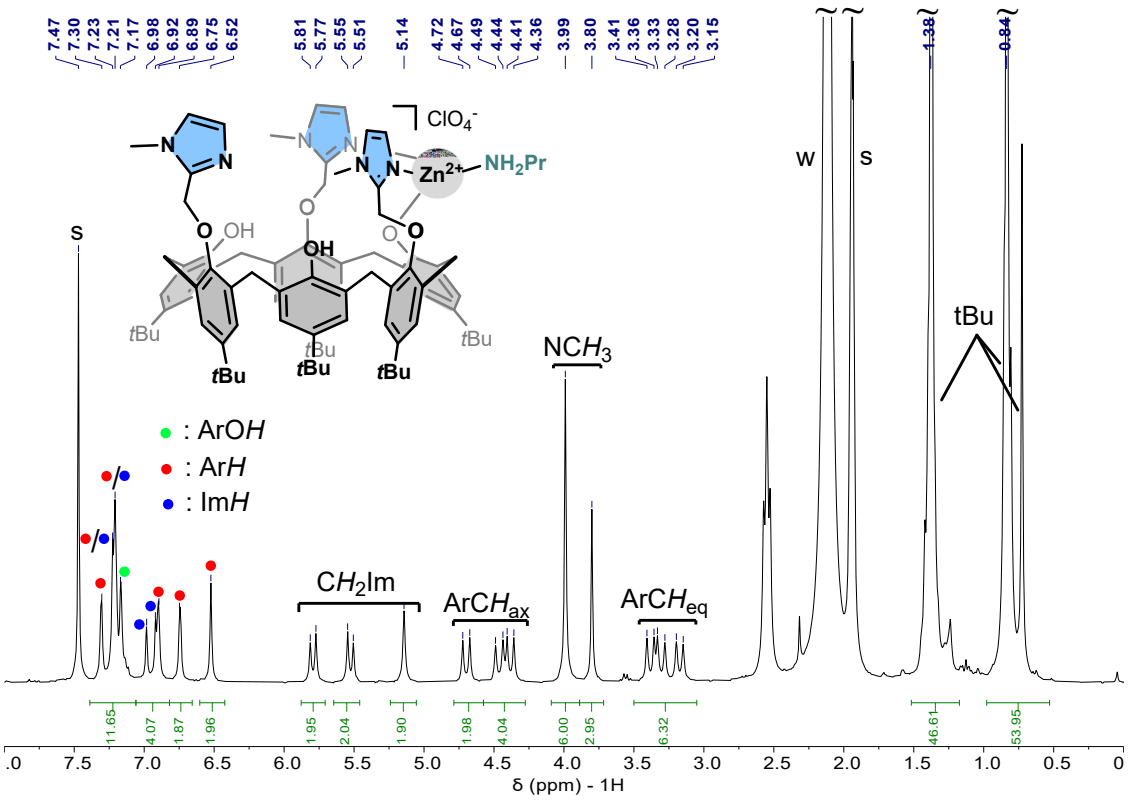

Figure SI20. ^{1}H NMR (298K, 500 MHz) spectrum of [Zn(**2**)(G)](ClO$_4$)$_2$ with 8 equiv. of propylamine in $CD_3CN/CDCl_3$ 1:1. S: solvent, w: water.

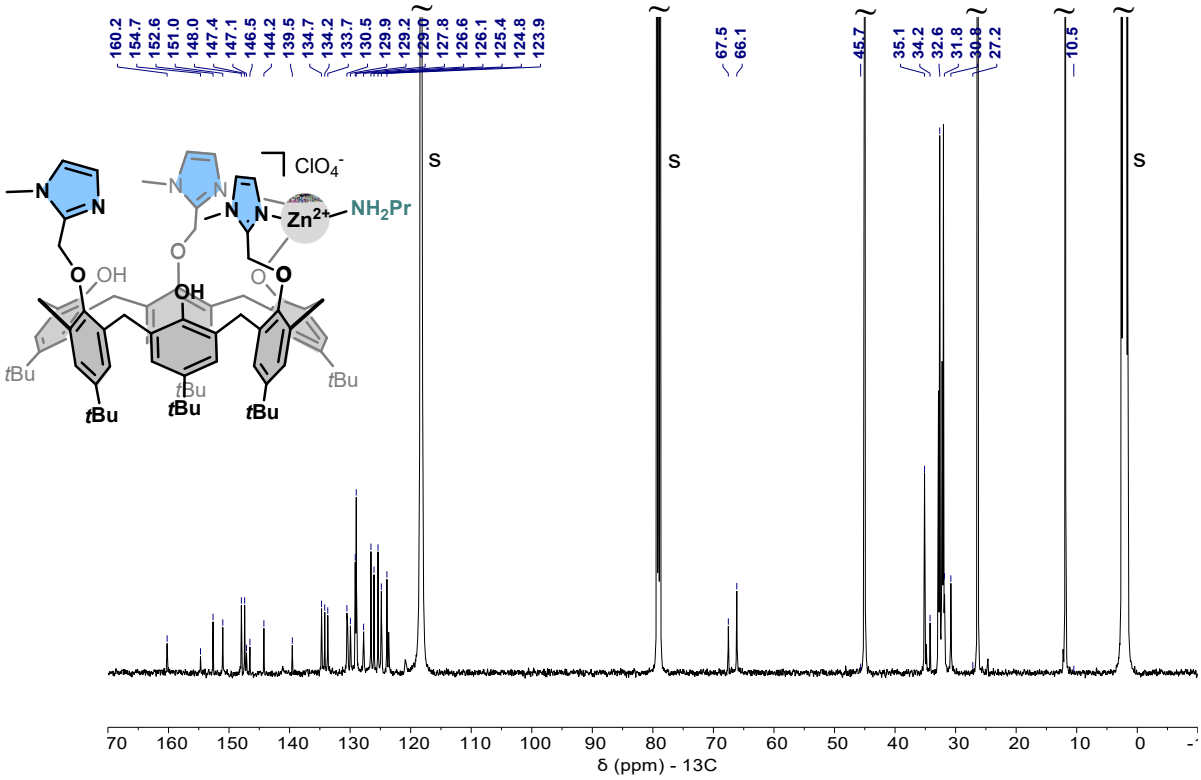

Figure SI21. ^{13}C NMR (298K, 126 MHz) spectrum of [Zn(**2**)(G)](ClO$_4$)$_2$ with 8 equiv. of propylamine in $CD_3CN/CDCl_3$ 1:1. S: solvent.

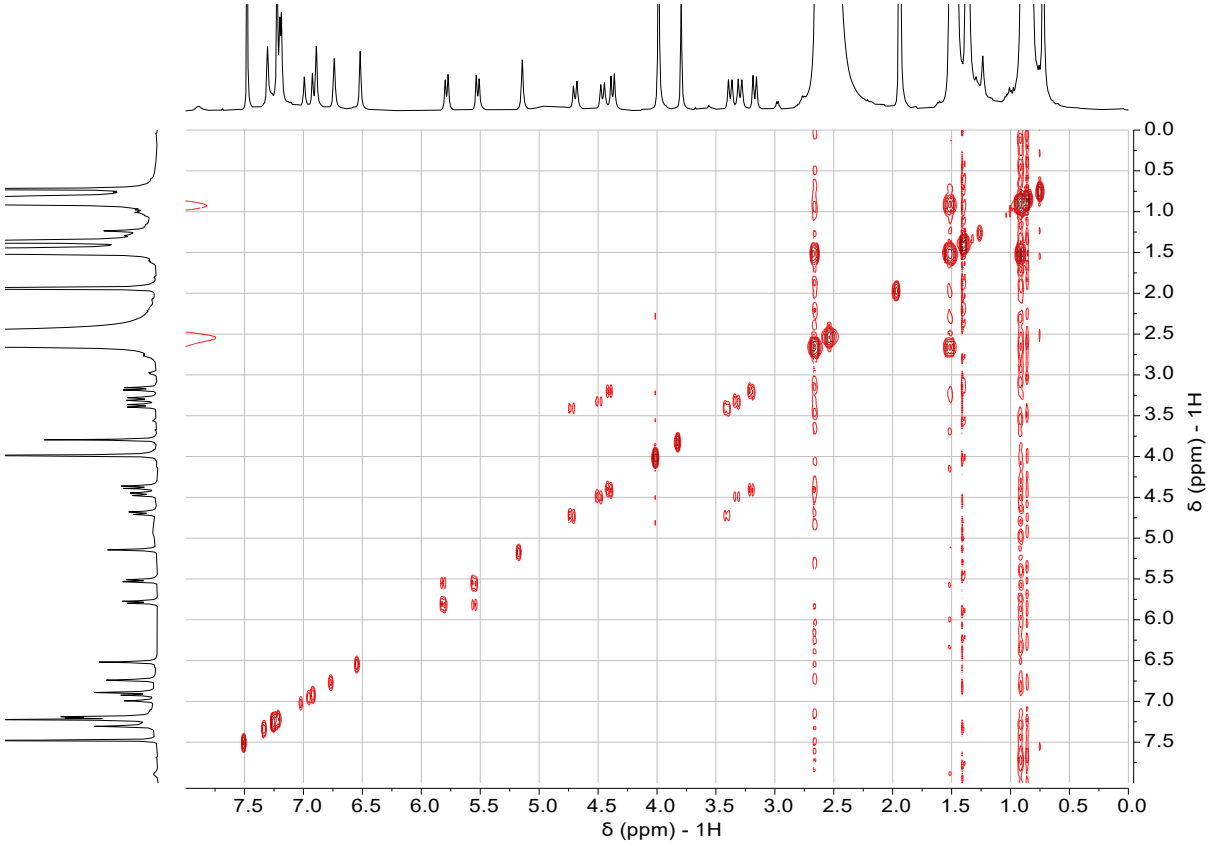

Figure SI22. COSY NMR (298K, 500 MHz) spectrum of [Zn(**2**)(G)]$(ClO_4)_2$ with 8 equiv. of propylamine in $CD_3CN/CDCl_3$ 1:1.

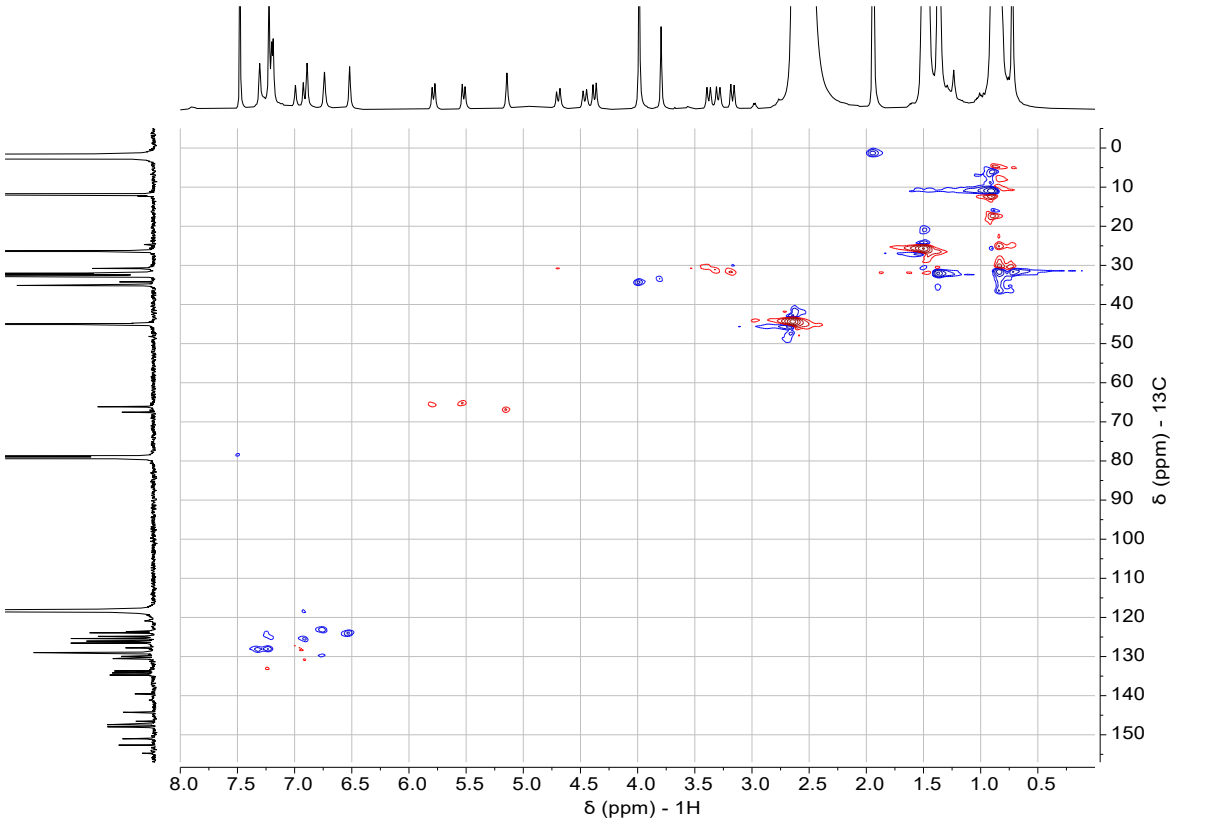

Figure SI23. HSQC NMR (298K, 500 MHz) spectrum of [Zn(**2**)(G)]$(ClO_4)_2$ with 8 equiv. of propylamine in $CD_3CN/CDCl_3$ 1:1.

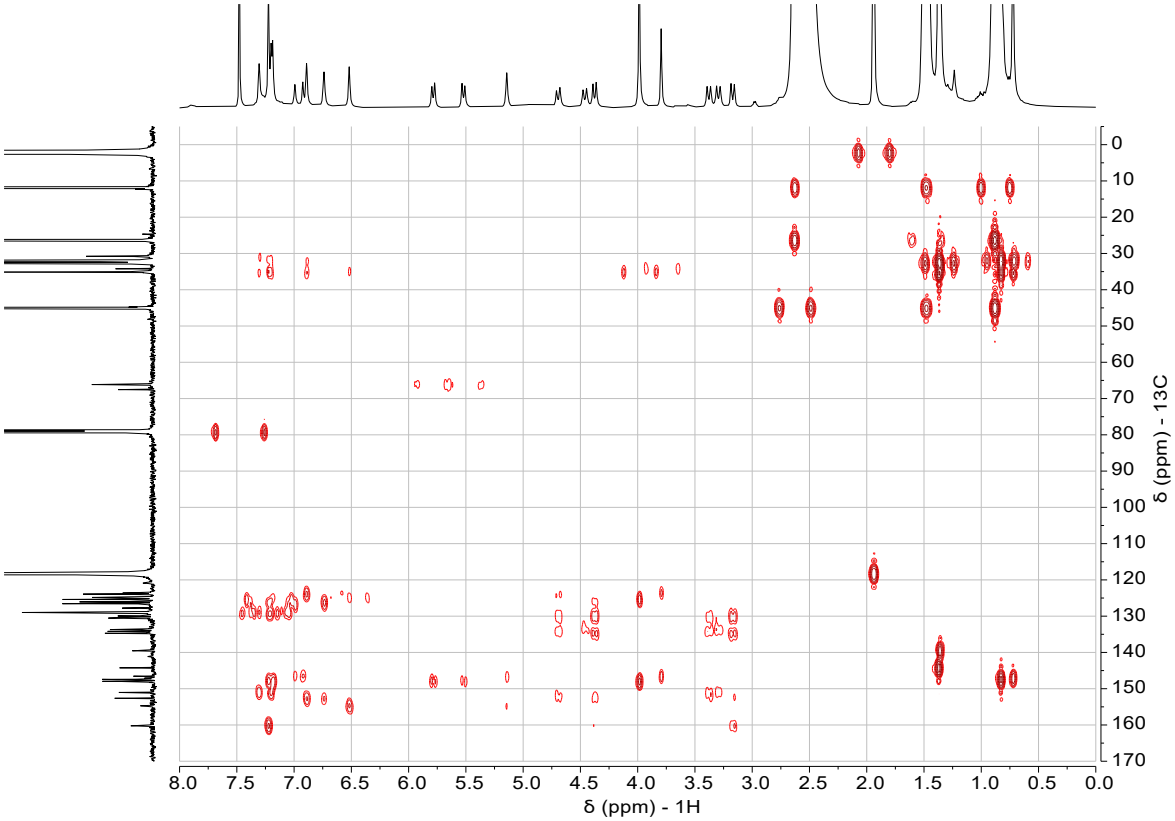

Figure SI24. HMBC NMR (298K, 500 MHz) spectrum of [Zn(**2**)(G)]$(ClO_4)_2$ with 8 equiv. of propylamine in $CD_3CN/CDCl_3$ 1:1.

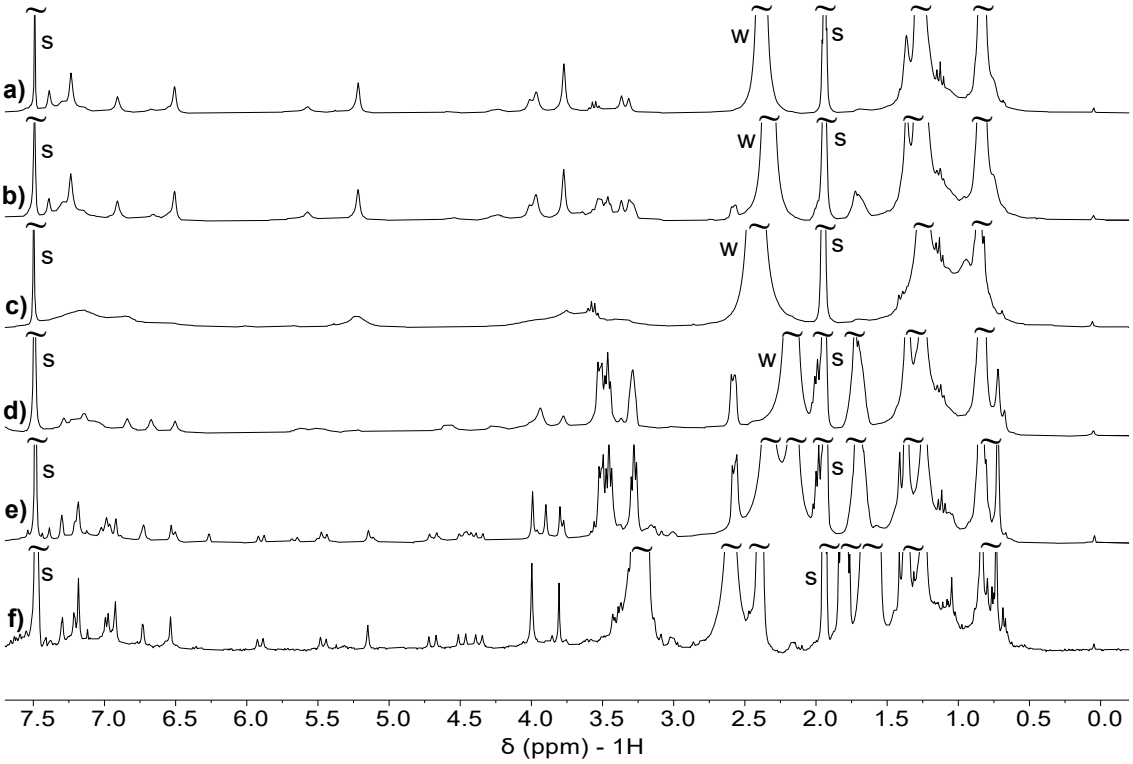

Figure SI25. ^1H NMR (298K, 300 MHz) titration showing the evolution of [Zn(**2**)(G)]$(ClO_4)_2$ in $CDCl_3/CD_3CN$1:1 by addition of a) before additions, b) 0.5 equiv. of DBU, c) 1 equiv. of DBU, d) 2 equiv. of DBU, e) 3 equiv. of DBU, f) 8 equiv. of DBU. S: solvent, w: water.

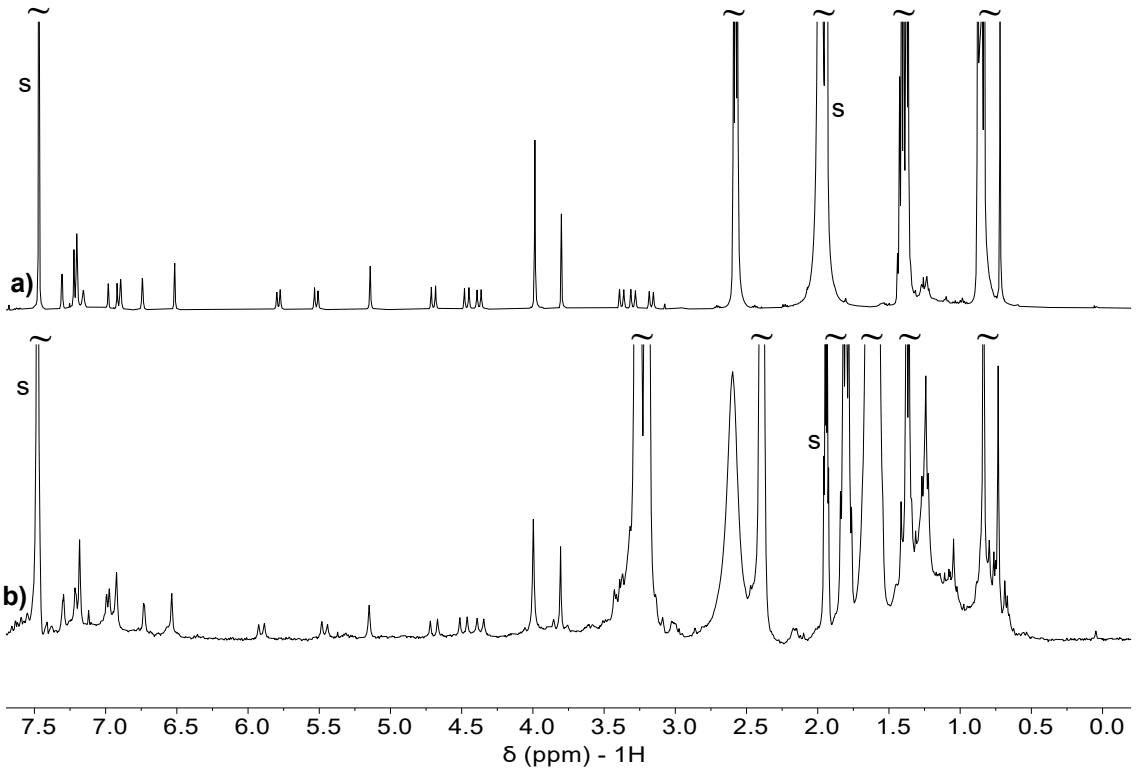

Figure SI26. ^{1}H NMR (298K, 500 MHz for a), 300 MHz for b)) of a) [Zn(**2**)(G)]$(ClO_4)_2$ with 8 equiv. of propylamine and b) [Zn(**2**)(G)]$(ClO_4)_2$ with 8 equiv. of DBU. S: solvent, w: water.

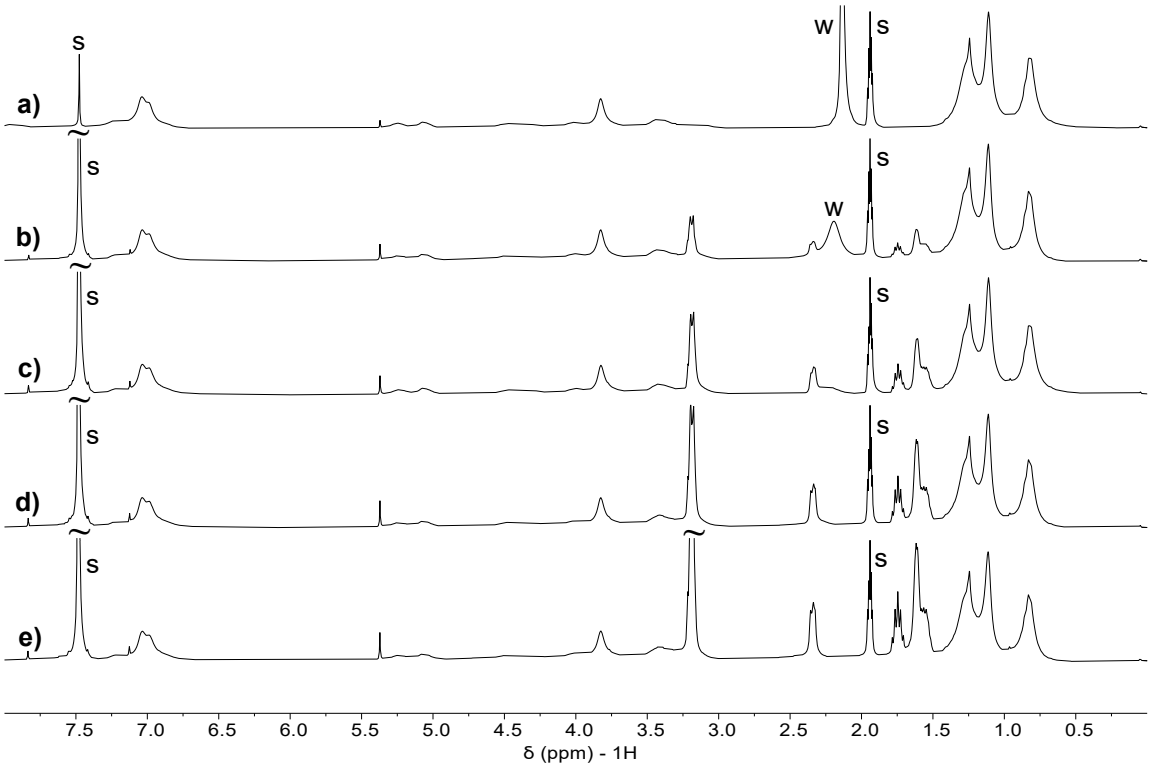

Figure SI27. ^{1}H NMR (298K, 300 MHz) titration showing the evolution of **2** in $CDCl_3/CD_3CN$ 1:1 by addition of a) before additions, b) 1 equiv. of DBU, c) 2 equiv. of DBU, d) 3 equiv. of DBU and e) 4 equiv. of DBU. S: solvent, w: water.

V. ^{1}H NMR spectra [Zn(**3**)(G)](ClO$_4$)$_2$ in CD$_3$CN/CDCl$_3$ 1:1 with addition of propylamine.

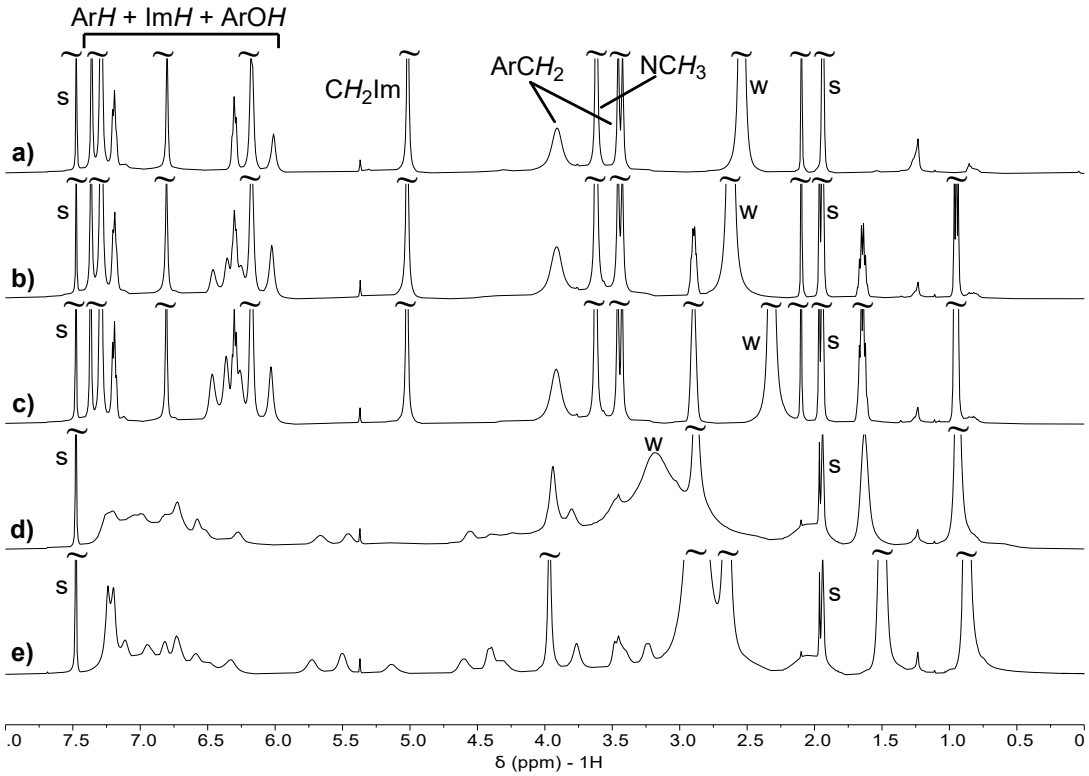

Figure SI28. ^{1}H NMR (298K, 500 MHz) titration showing the evolution of [Zn(**3**)(G)](ClO$_4$)$_2$ in CDCl$_3$/CD$_3$CN 1:1 v:v by addition of a) before additions, b) 1 equiv. of propylamine, c) 2 equiv. of propylamine, d) 3 equiv. of propylamine and e) 8 equiv. of propylamine. S: solvent, w: water.

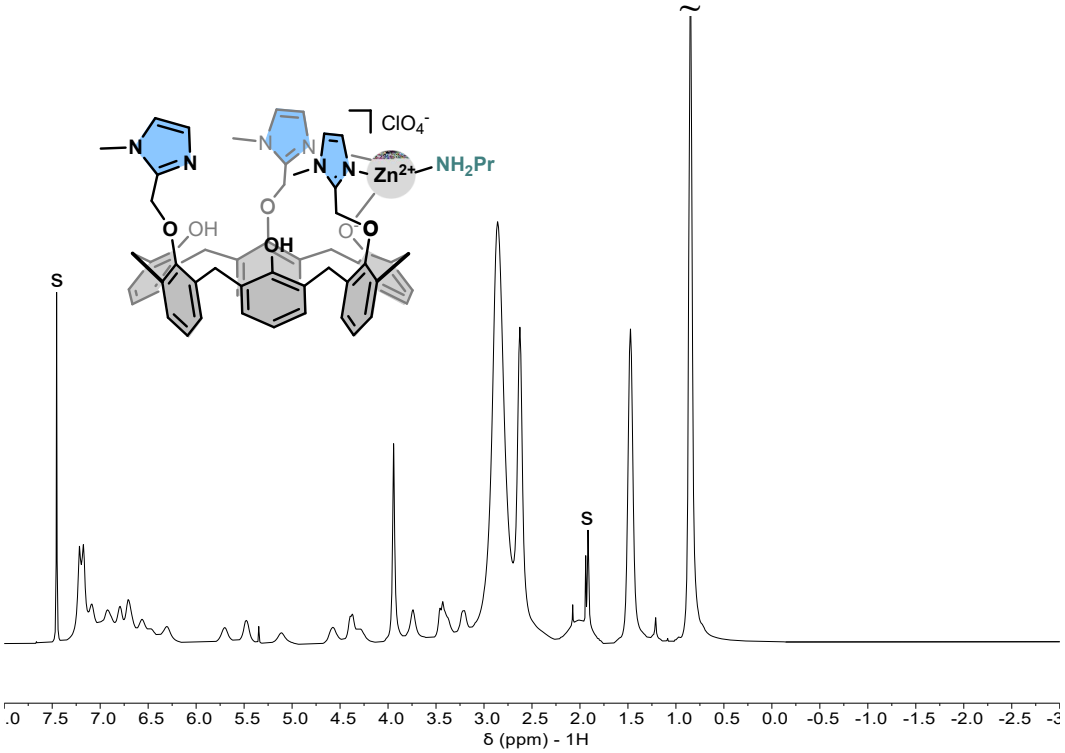

Figure SI29. ^{1}H NMR (298K, 500 MHz) spectrum of **[Zn(3)(G)](ClO$_4$)$_2$** with 8 equiv. of propylamine in

$CD_3CN/CDCl_3$ 1:1. S: solvent.

VI. ^1H NMR, ^{13}C NMR, COSY NMR, HSQC NMR and HMBC NMR $[Zn(\mathbf{2})(G)](ClO_4)_2$ in $CD_3CN/CDCl_3$ 1:1 with addition of tetrabutylammonium acetate.

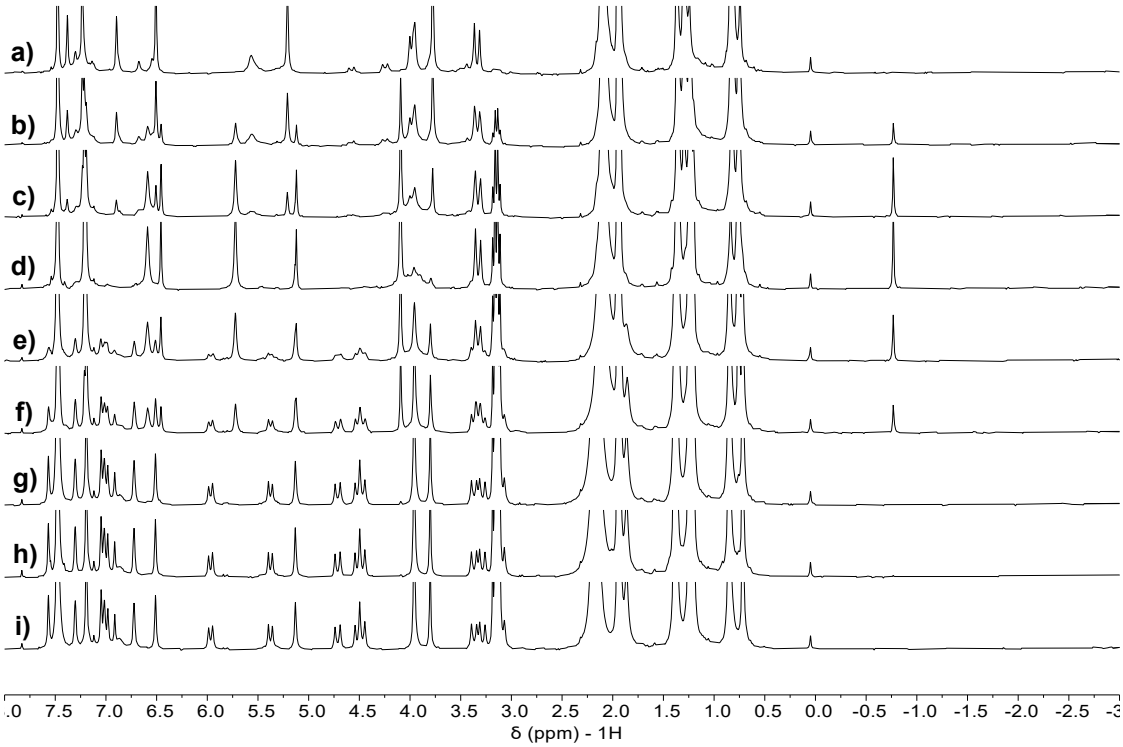

Figure SI30. ^1H NMR (298K, 400 MHz) titration showing the evolution of $[Zn(\mathbf{2})(G)](ClO_4)_2$ in $CDCl_3/CD_3CN$ 1:1 by addition of a) before additions, b) 0.3 equiv. of TBAacetate, c) 0.6 equiv. of TBAacetate, d) 1 equiv. of TBAacetate, e) 1.4 equiv. of TBAacetate, f) 1.8 equiv. of TBAacetate, g) 2.2 equiv. of TBAacetate, h) 2.6 equiv. of TBAacetate and i) 3 equiv. of TBAacetate.

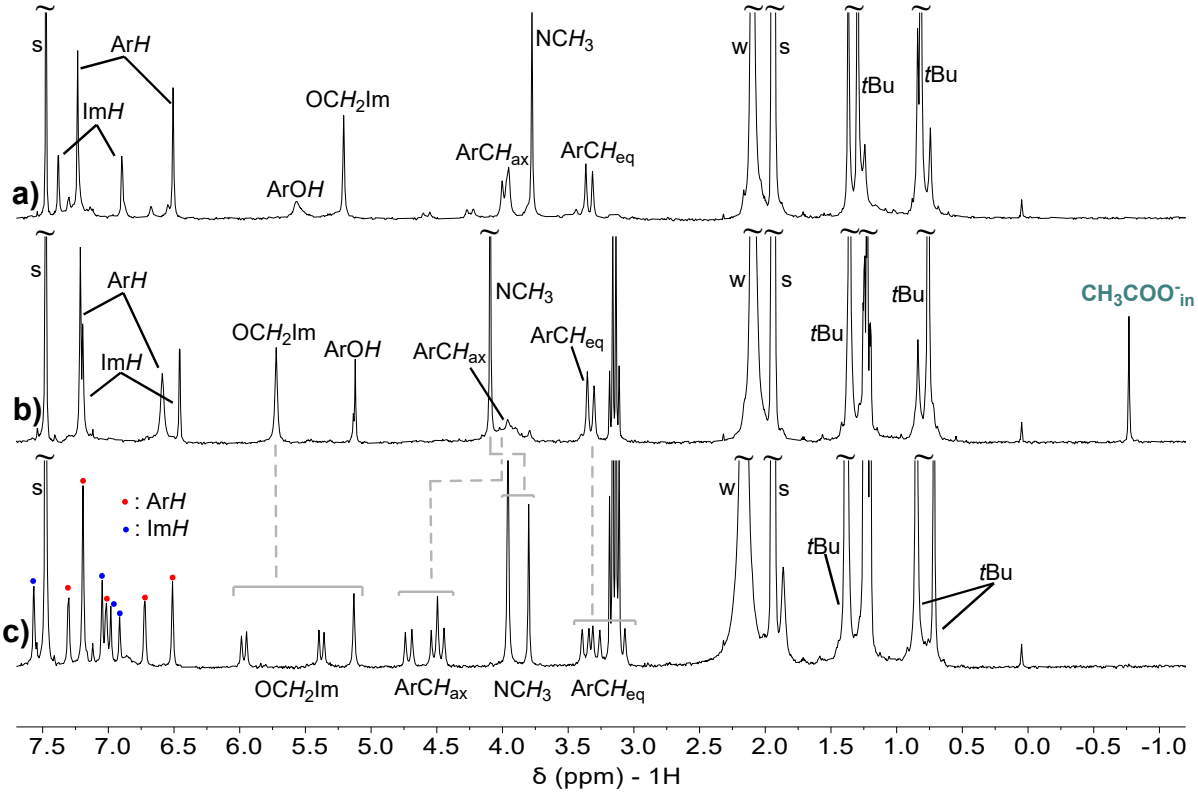

Figure SI31. ^{1}H NMR (298K, 400 MHz) titration showing the evolution of [Zn(**2**)(G)](ClO$_4$)$_2$ in CDCl$_3$/CD$_3$CN 1:1 by addition of a) before additions, b) 1 equiv. of TBAacetate and c) 2.2 equiv. of TBAacetate. S: solvent, w: water.

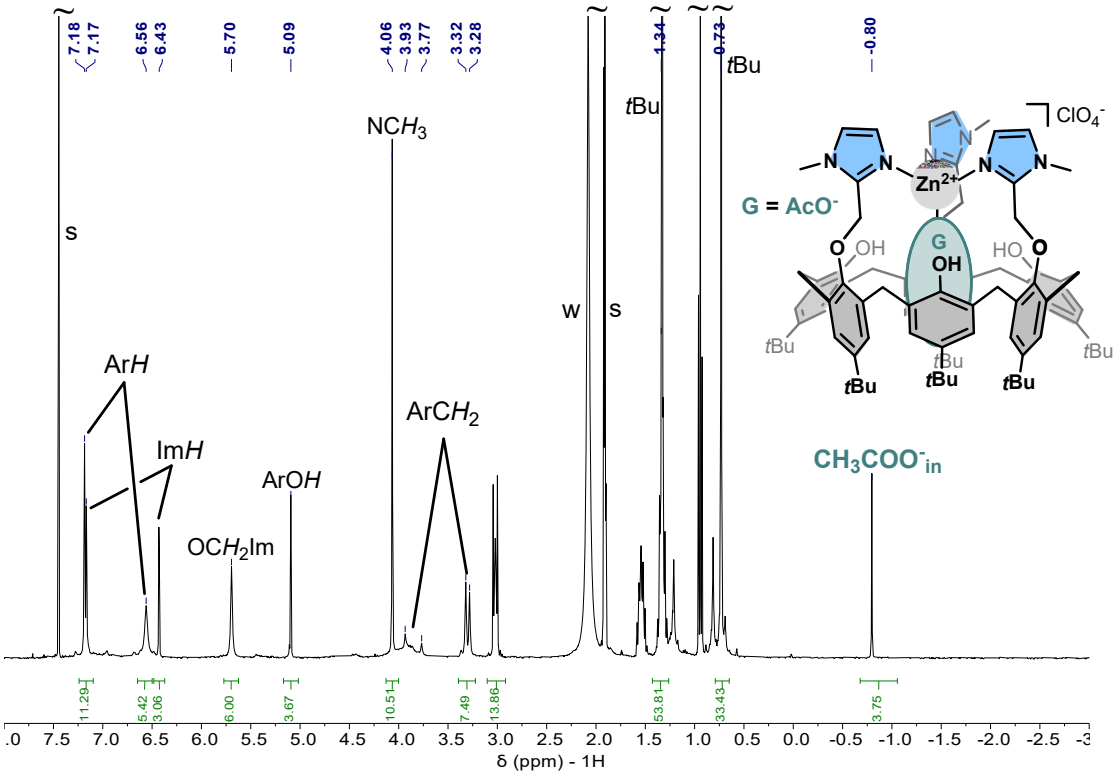

Figure SI32. ^{1}H NMR (298K, 500 MHz) spectrum of [Zn(**2**)(G)](ClO$_4$)$_2$ with 1 equiv. of TBAacetate in CD$_3$CN/CDCl$_3$ 1:1. S: solvent, w: water.

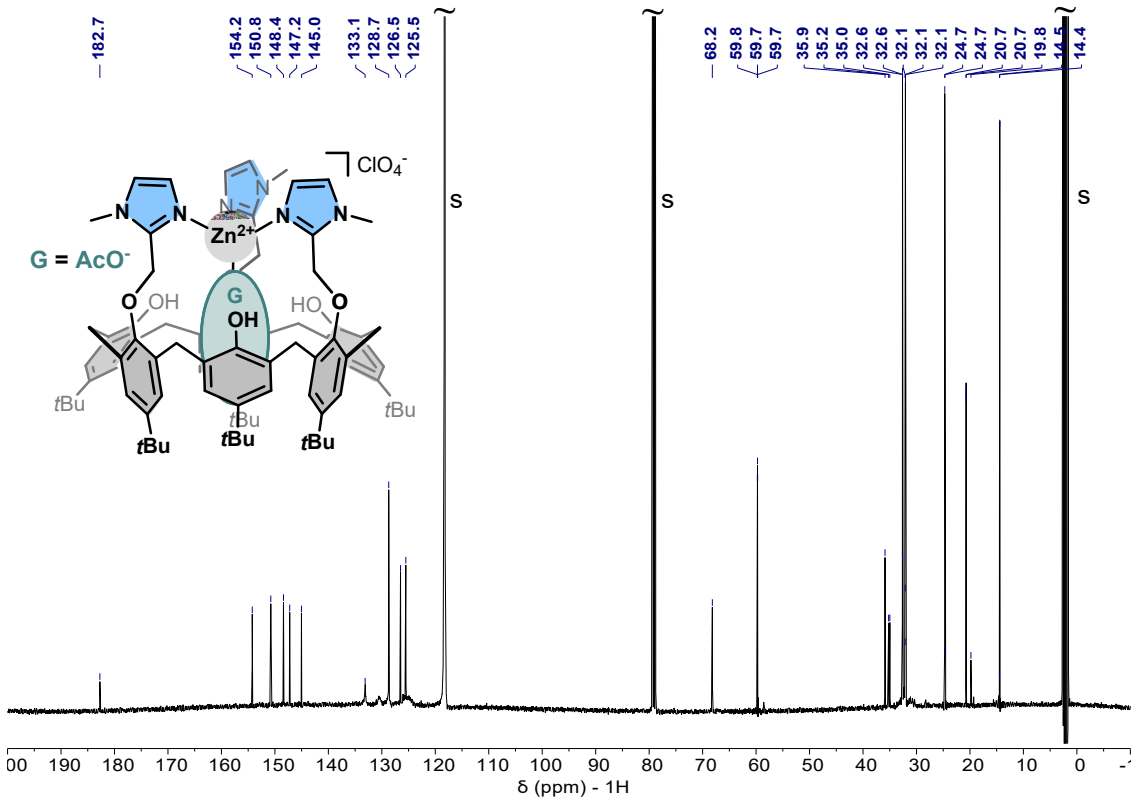

Figure SI33. ^{13}C NMR (298K, 126 MHz) spectrum of [Zn(**2**)(G)]$(ClO_4)_2$ with 1 equiv. of TBAacetate in $CD_3CN/CDCl_3$ 1:1. S: solvent.

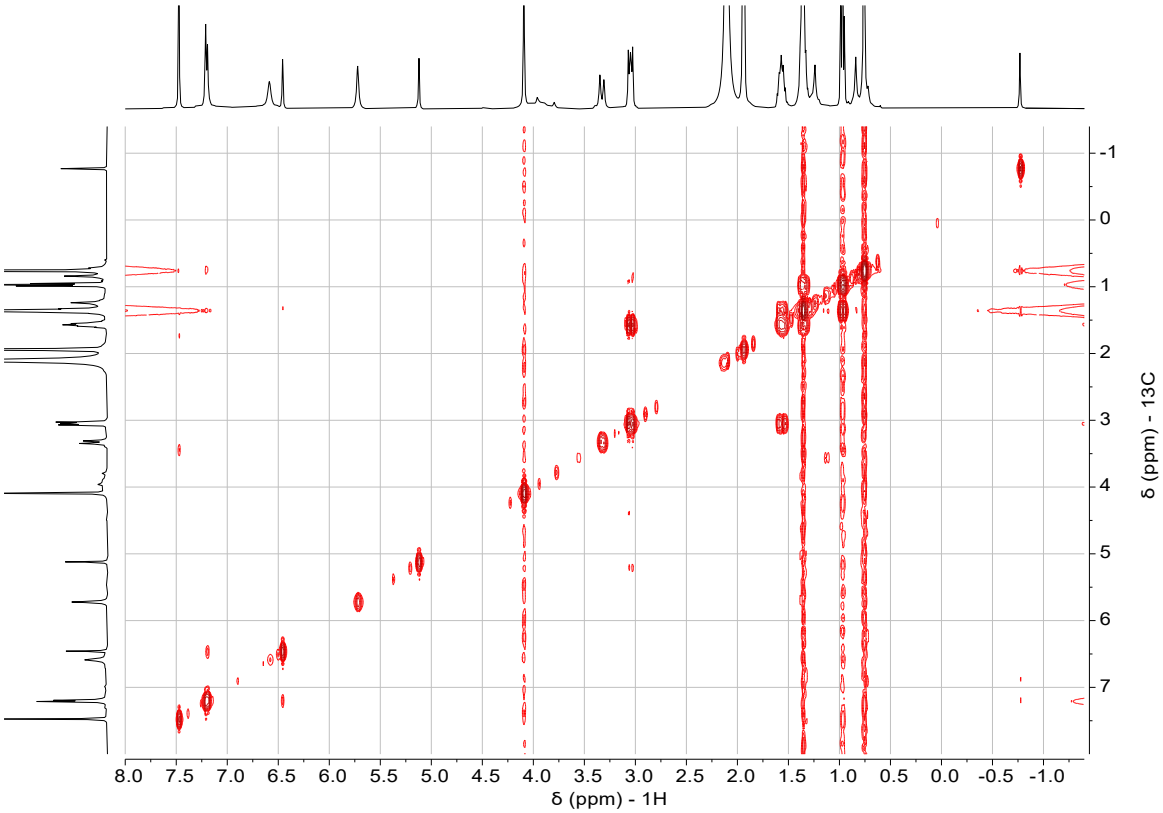

Figure SI34. COSY NMR (298K, 500 MHz) spectrum of [Zn(**2**)(G)]$(ClO_4)_2$ with 1 equiv. of TBAacetate in $CD_3CN/CDCl_3$ 1:1.

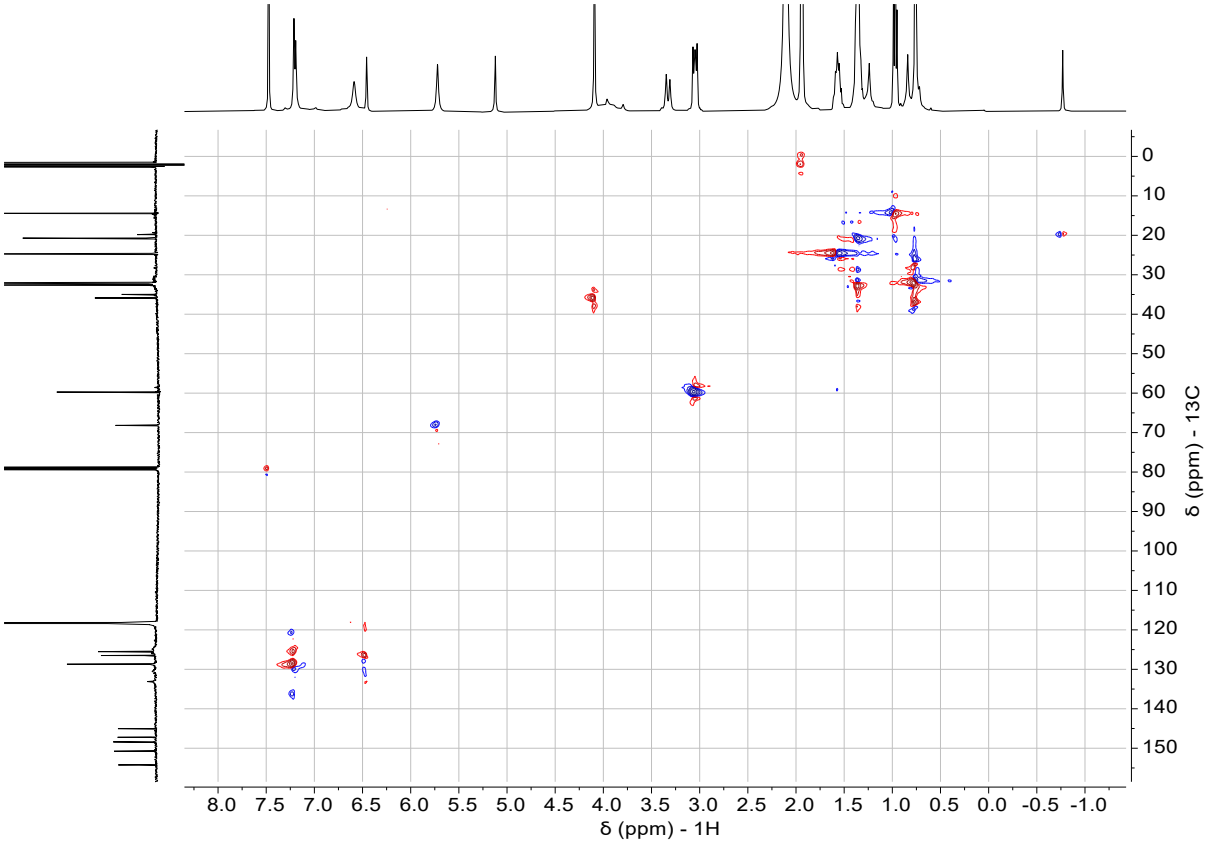

Figure SI35. HSQC NMR (298K, 500 MHz) spectrum of [Zn(**2**)(G)]$(ClO_4)_2$ with 1 equiv. of TBAacetate in $CD_3CN/CDCl_3$ 1:1.

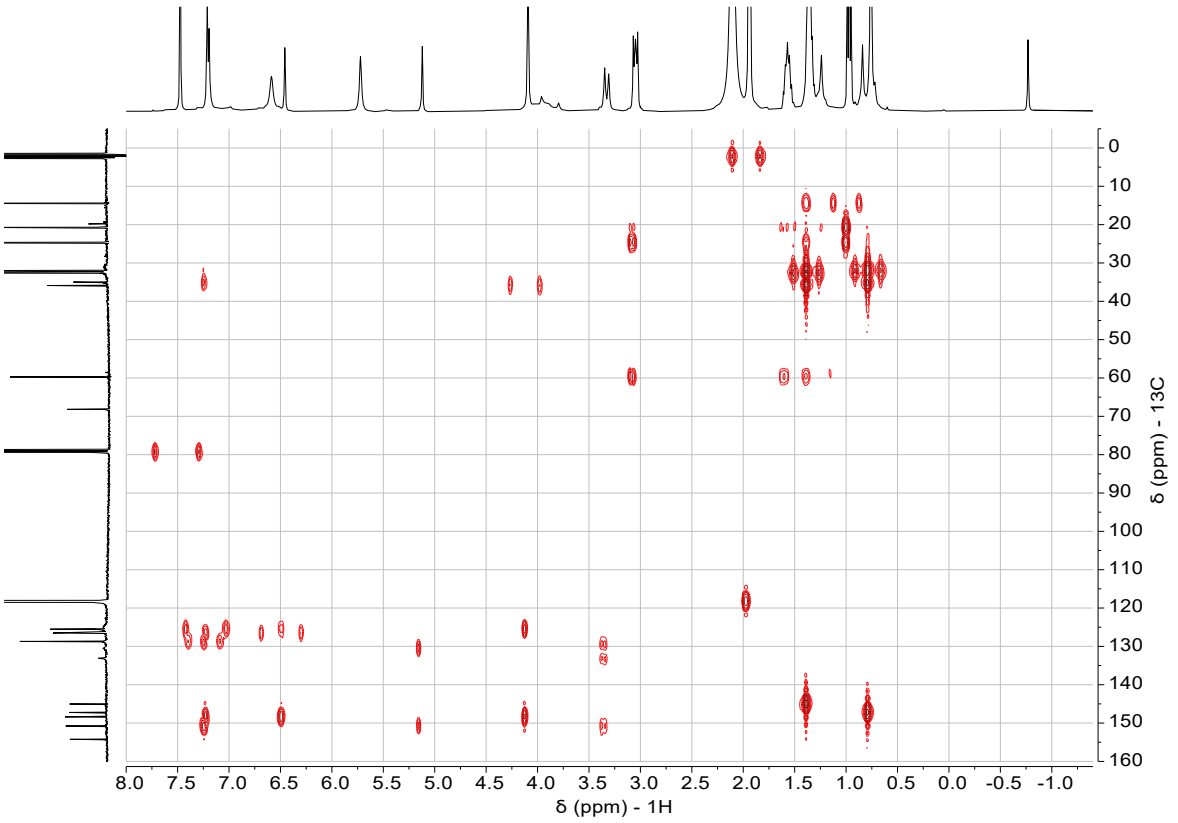

Figure SI36. HMBC NMR (298K, 500 MHz) spectrum of [Zn(**2**)(G)]$(ClO_4)_2$ with 1 equiv. of TBAacetate in $CD_3CN/CDCl_3$ 1:1.

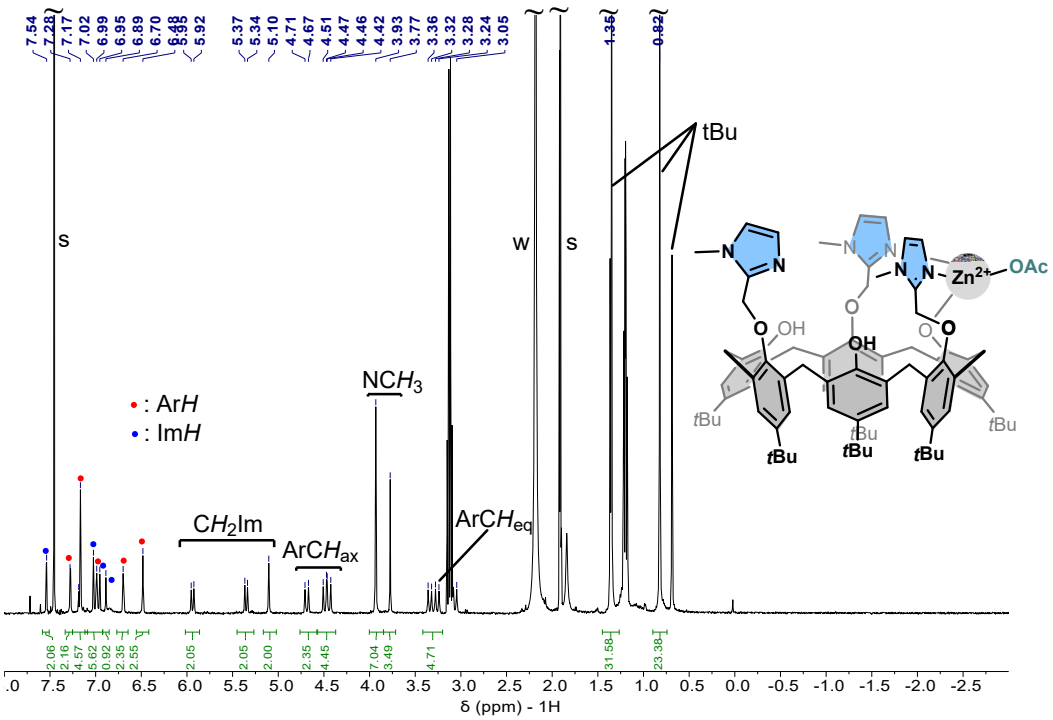

Figure SI37. ^{1}H NMR (298K, 400 MHz) spectrum of [Zn(**2**)(G)](ClO$_4$)$_2$ with 3 equiv. of TBAacetate in CD$_3$CN/CDCl$_3$ 1:1. S: solvent, w: water.

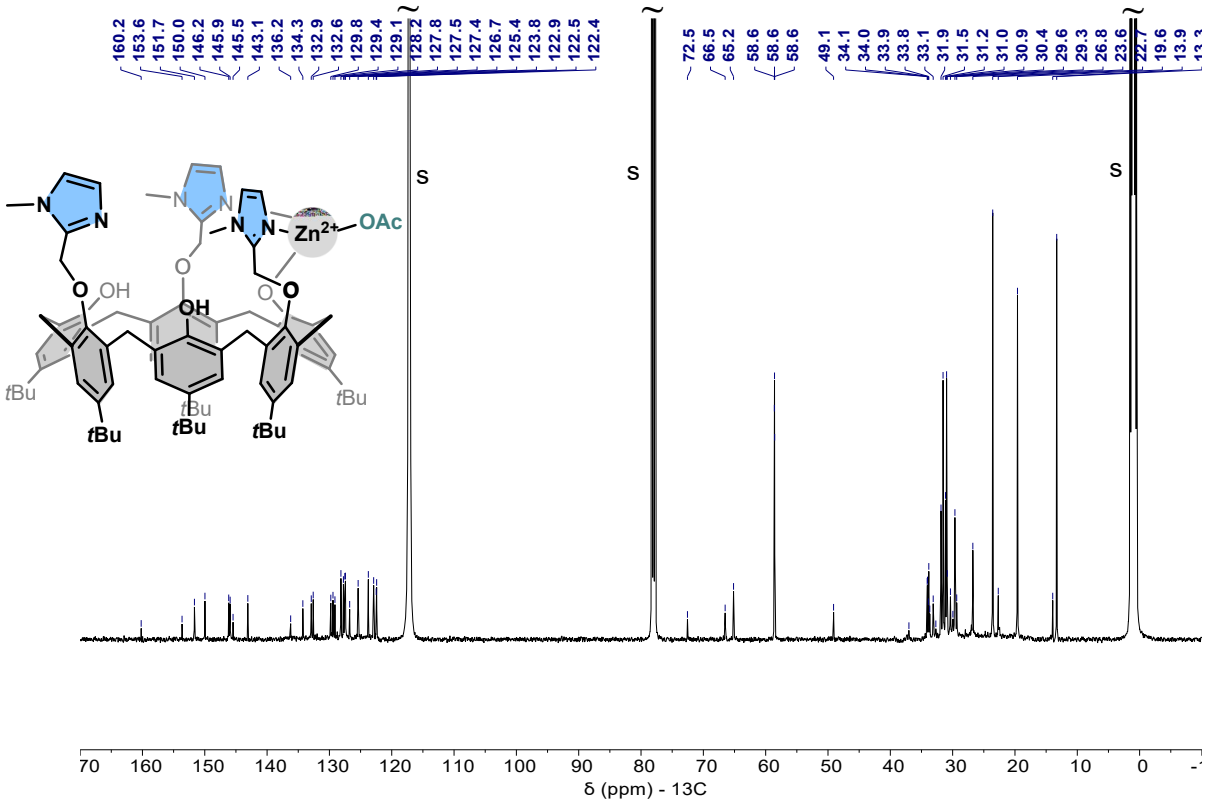

Figure SI38. ^{13}C NMR (298K, 100 MHz) spectrum of [Zn(**2**)(G)](ClO$_4$)$_2$ with 3 equiv. of TBAacetate in CD$_3$CN/CDCl$_3$ 1:1. S: solvent.

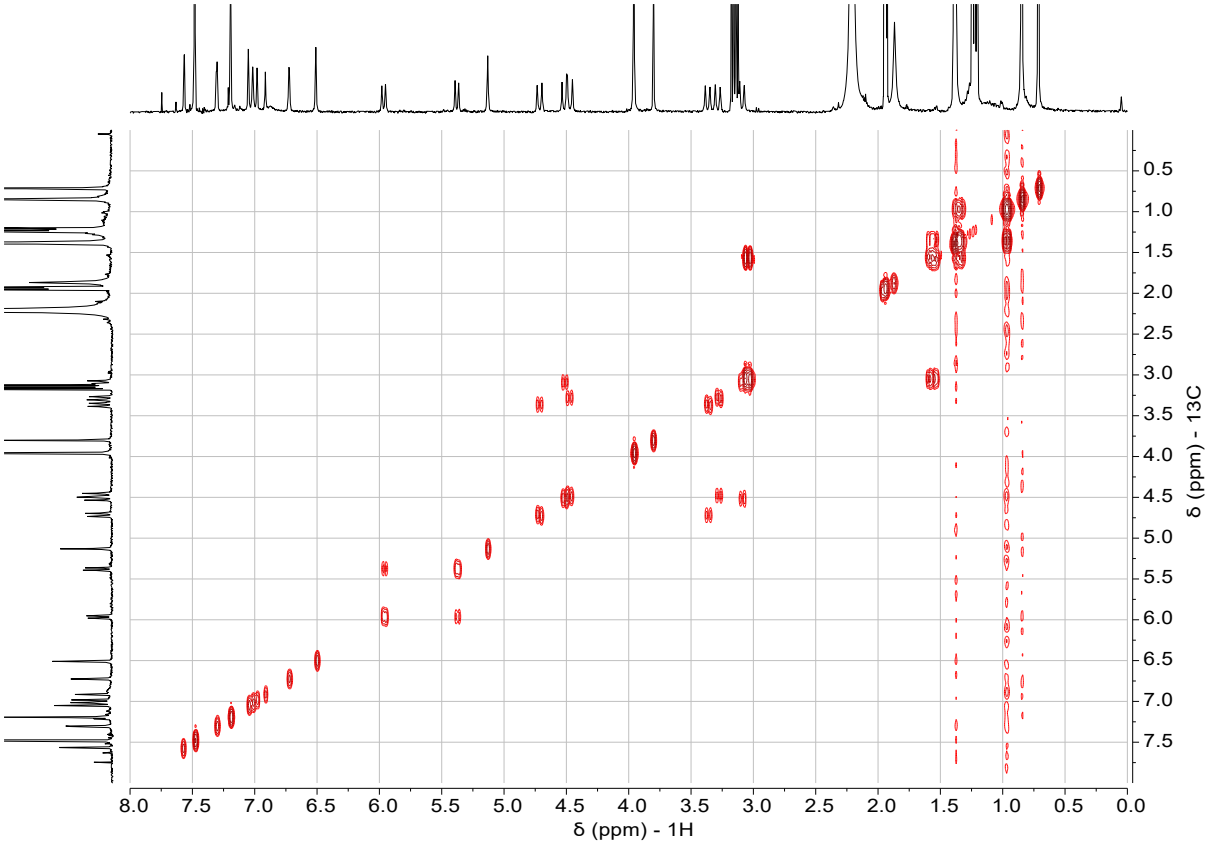

Figure SI39. COSY NMR (298K, 400 MHz) spectrum of [Zn(**2**)(G)]$(ClO_4)_2$ with 3 equiv. of TBAacetate in $CD_3CN/CDCl_3$ 1:1.

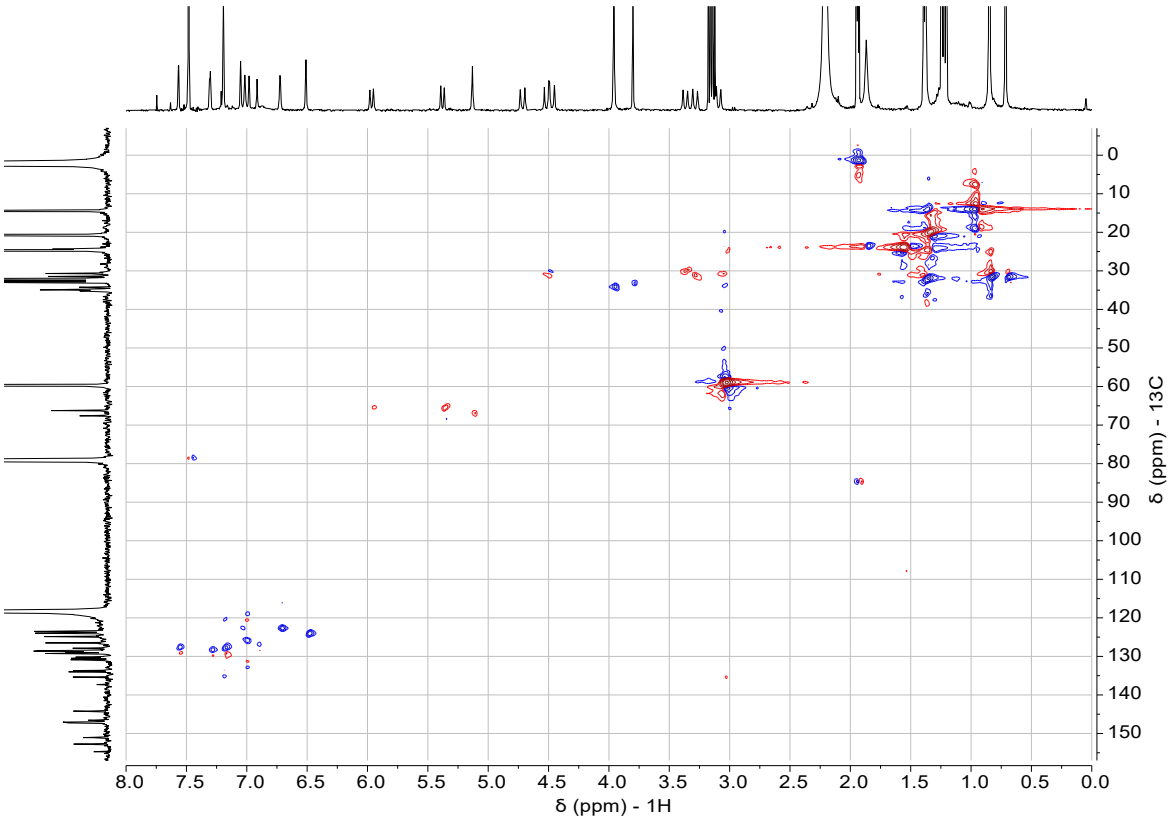

Figure SI40. HSQC NMR (298K, 400 MHz) spectrum of [Zn(**2**)(G)]$(ClO_4)_2$ with 3 equiv. of TBAacetate in $CD_3CN/CDCl_3$ 1:1.

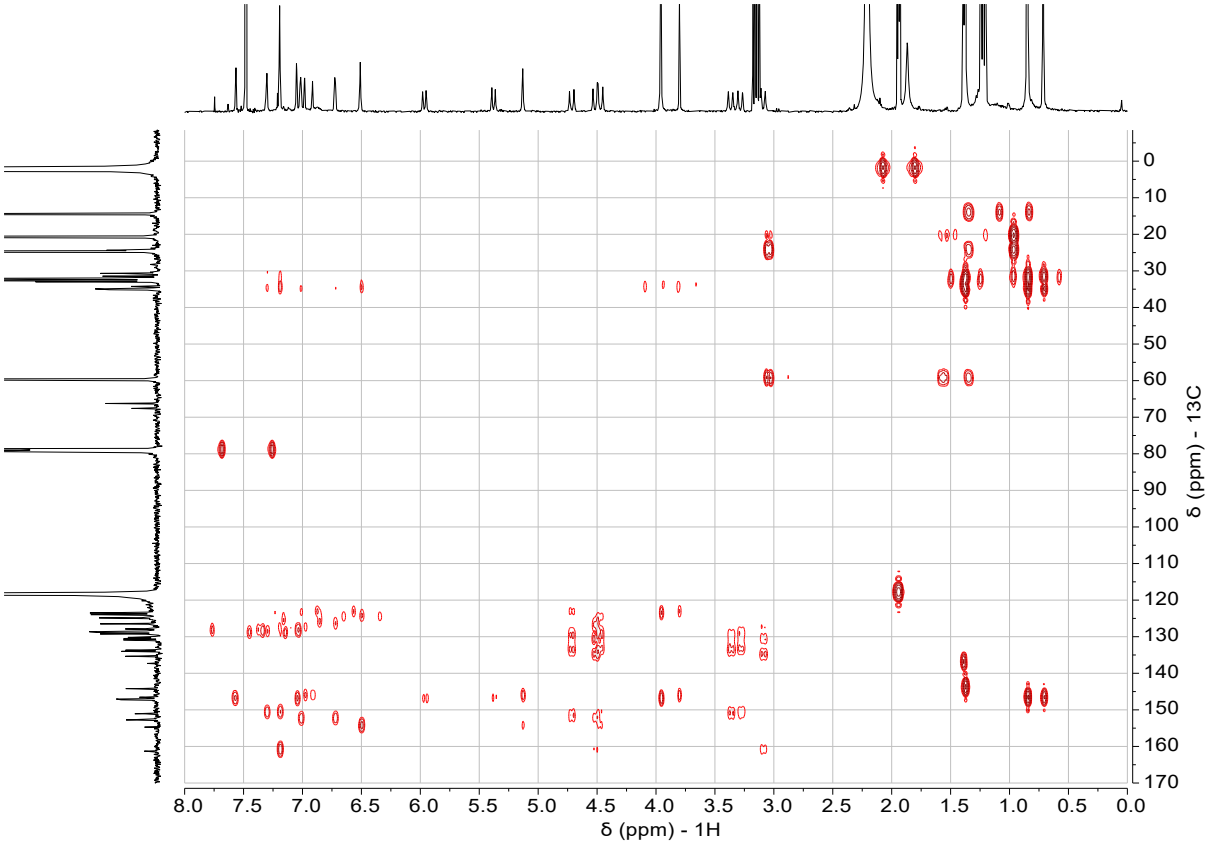

Figure SI41. HMBC NMR (298K, 400 MHz) spectrum of [Zn(**2**)(G)]$(ClO_4)_2$ with 3 equiv. of TBAacetate in $CD_3CN/CDCl_3$ 1:1.

VII. ^{1}H NMR, ^{13}C NMR, COSY NMR, HSQC NMR and HMBC NMR [Zn(**3**)(G)](ClO$_4$)$_2$ in $CD_3CN/CDCl_3$ 1:1 with addition of tetrabutylammonium acetate.

The behaviour of [Zn(**3**)(CH_3CN)](ClO$_4$)$_2$ toward acetate was next investigated. The process, monitored by ^{1}H NMR, also proceeds in two stages: initial recognition of the acetate anion, followed by deprotonation of the receptor (Figures SI42-SI44). The spectra of both the intermediate monocationic complex [Zn(**3**)(OAc)](ClO$_4$) (1 equiv. of acetate) and the final deprotonated species (2 equiv. of acetate) appeared broadened at 298 K, as previously observed during deprotonation with propylamine (Figure SI28). However, at 238 K, the signals sharpened significantly and enabled unambiguous structural assignment (Figures SI45-SI51). Comparison with the spectra recorded for [Zn(**2**)(CH_3CN)](ClO$_4$)$_2$ advocate for the same behaviour in the presence of acetate.

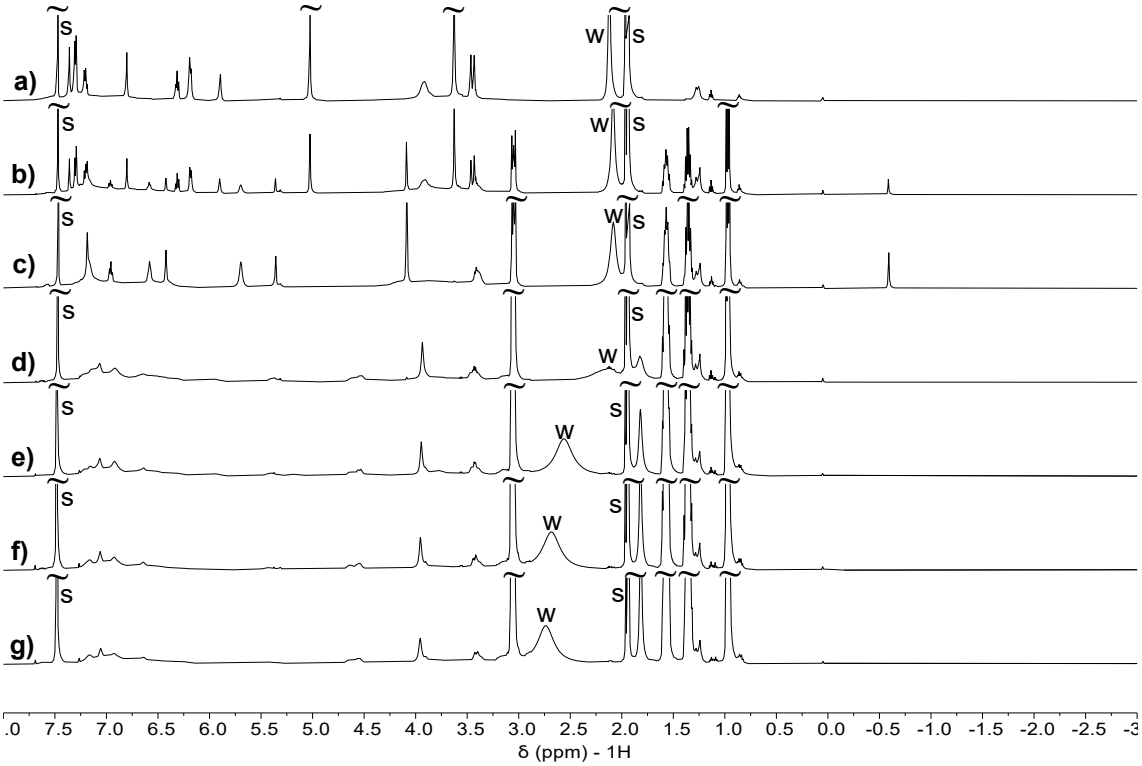

Figure SI42. ^{1}H NMR (298K, 400 MHz) titration showing the evolution of [Zn(**3**)(G)](ClO$_4$)$_2$ in $CDCl_3/CD_3CN$ 1:1 by addition of a) before additions, b) 0.5 equiv. of TBAacetate, c) 1 equiv. of TBAacetate, d) 2 equiv. of TBAacetate, e) 3 equiv. of TBAacetate, f) 4 equiv. of TBAacetate and g) 5 equiv. of TBAacetate.

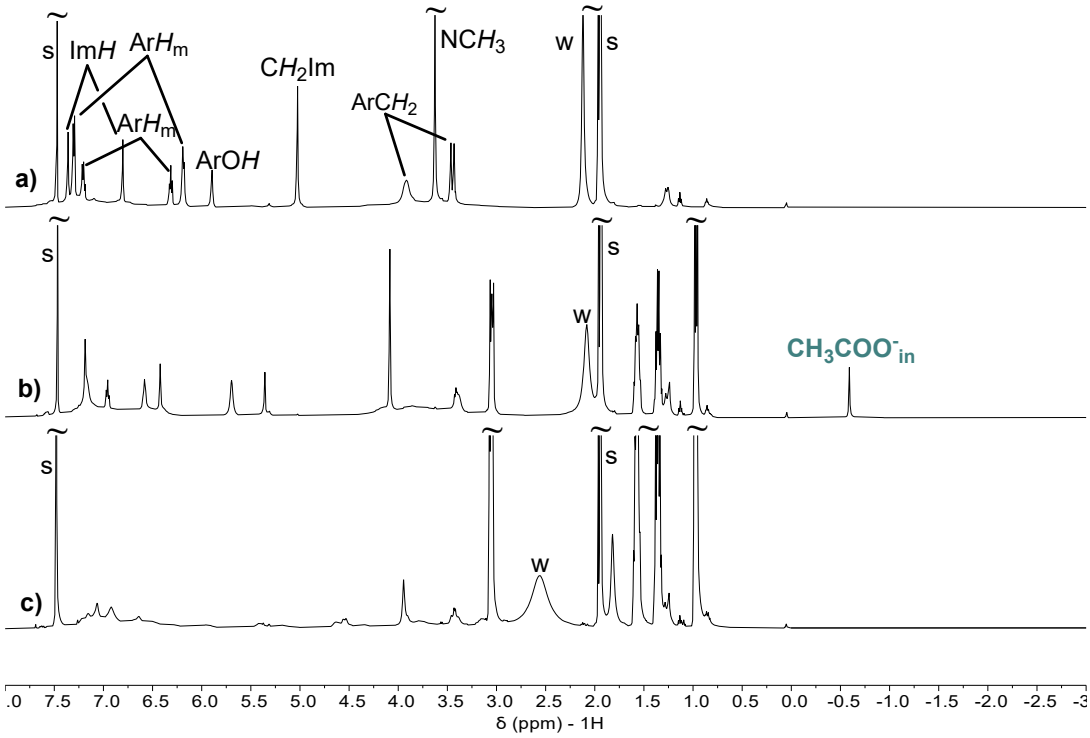

Figure SI43. ^{1}H NMR (298K, 400 MHz) titration showing the evolution of [Zn(**3**)(G)](ClO$_4$)$_2$ in CDCl$_3$/CD$_3$CN 1:1 by addition of a) before additions, b) 1 equiv. of TBAacetate and c) 3 equiv. of TBAacetate. S: solvent, w: water.

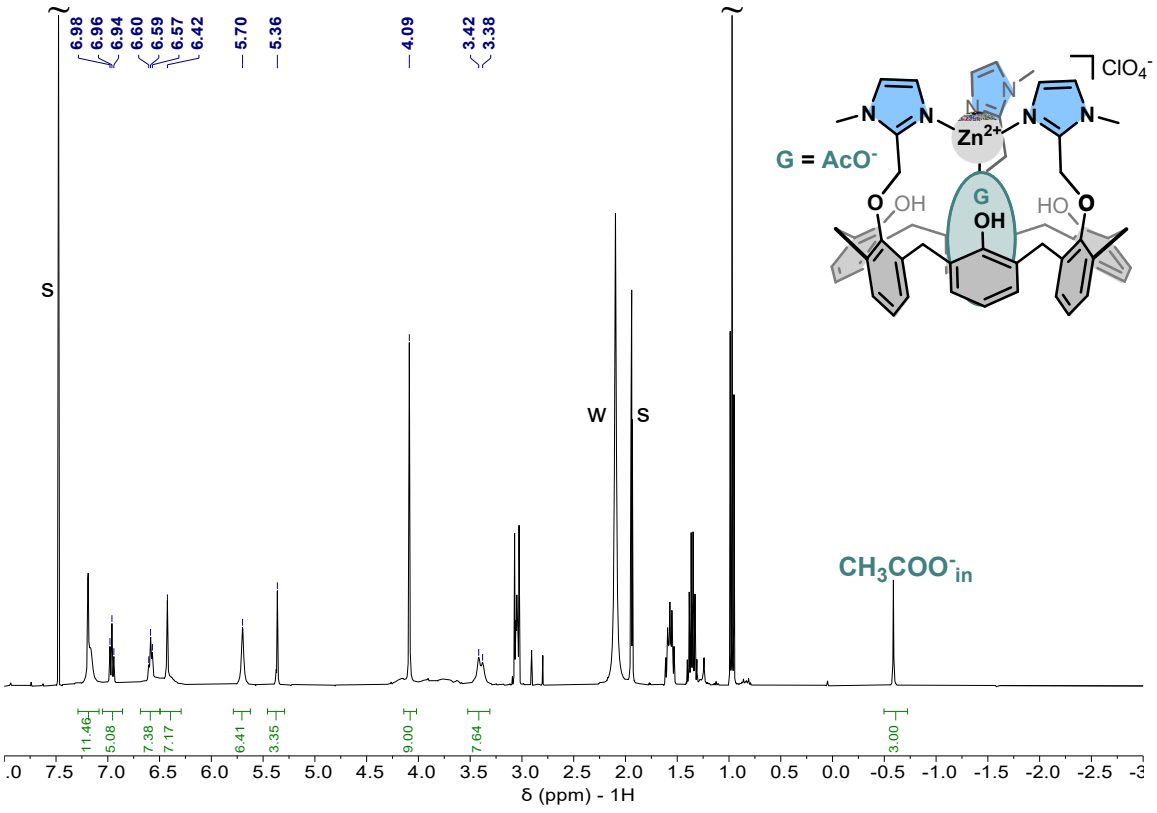

Figure SI44. ^{1}H NMR (298K, 400 MHz) spectrum of [Zn(**3**)(G)](ClO$_4$)$_2$ with 1 equiv. of TBAacetate in CD$_3$CN/CDCl$_3$ 1:1. S: solvent, w: water.

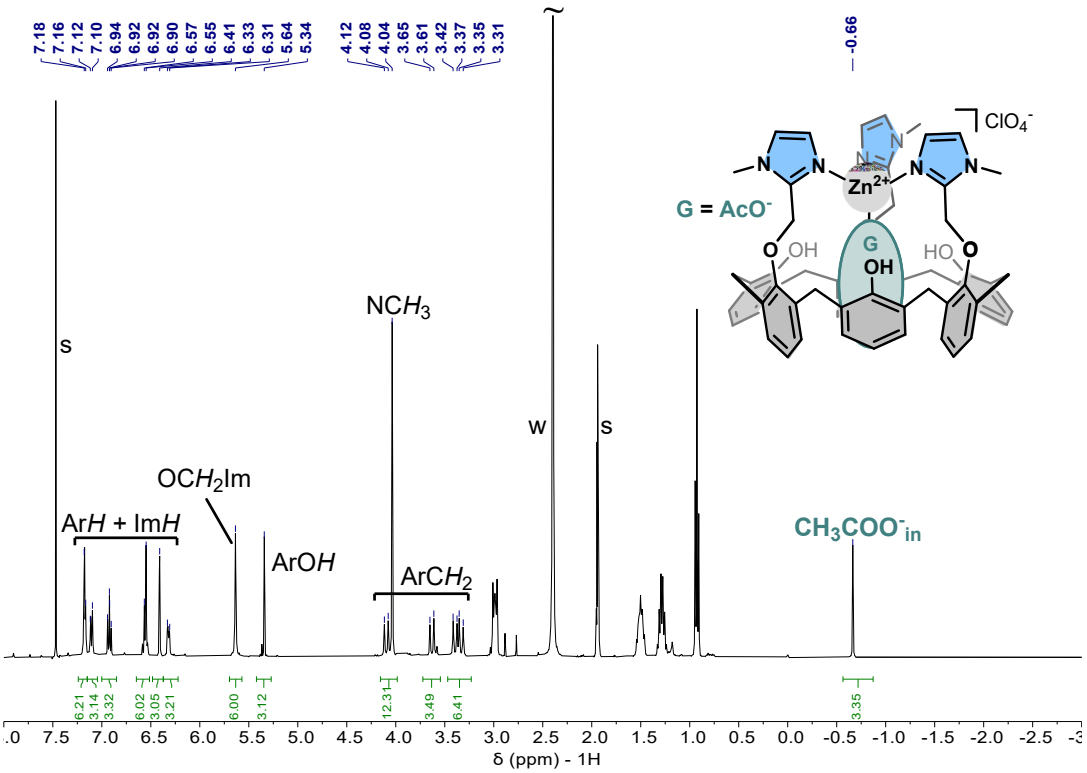

Figure SI45. ^{1}H NMR (238K, 400 MHz) spectrum of [Zn(**3**)(G)](ClO$_4$)$_2$ with 1 equiv. of TBAacetate in $CD_3CN/CDCl_3$ 1:1. S: solvent, w: water.

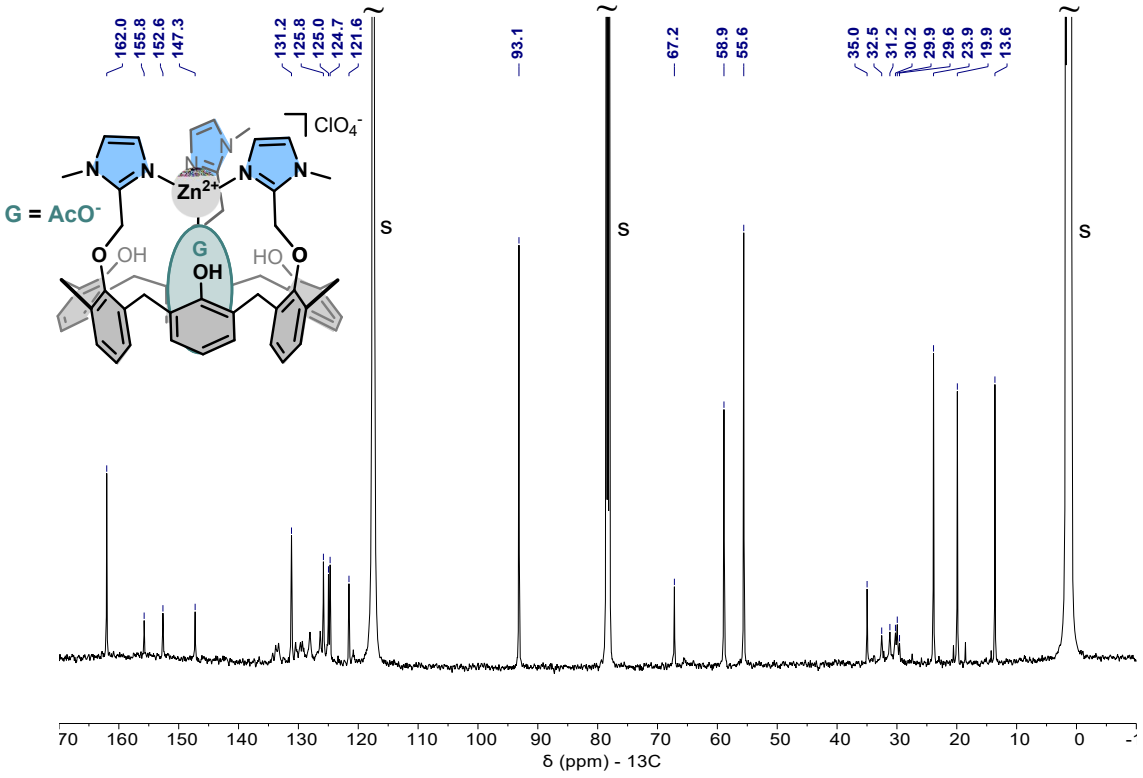

Figure SI46. ^{13}C NMR (298K, 100 MHz) spectrum of [Zn(**3**)(G)](ClO$_4$)$_2$ with 1 equiv. of TBAacetate in $CD_3CN/CDCl_3$ 1:1. S: solvent. Additional note: The spectrum was not recorded at 238 K, as it would have required long acquisition time at low temperature.

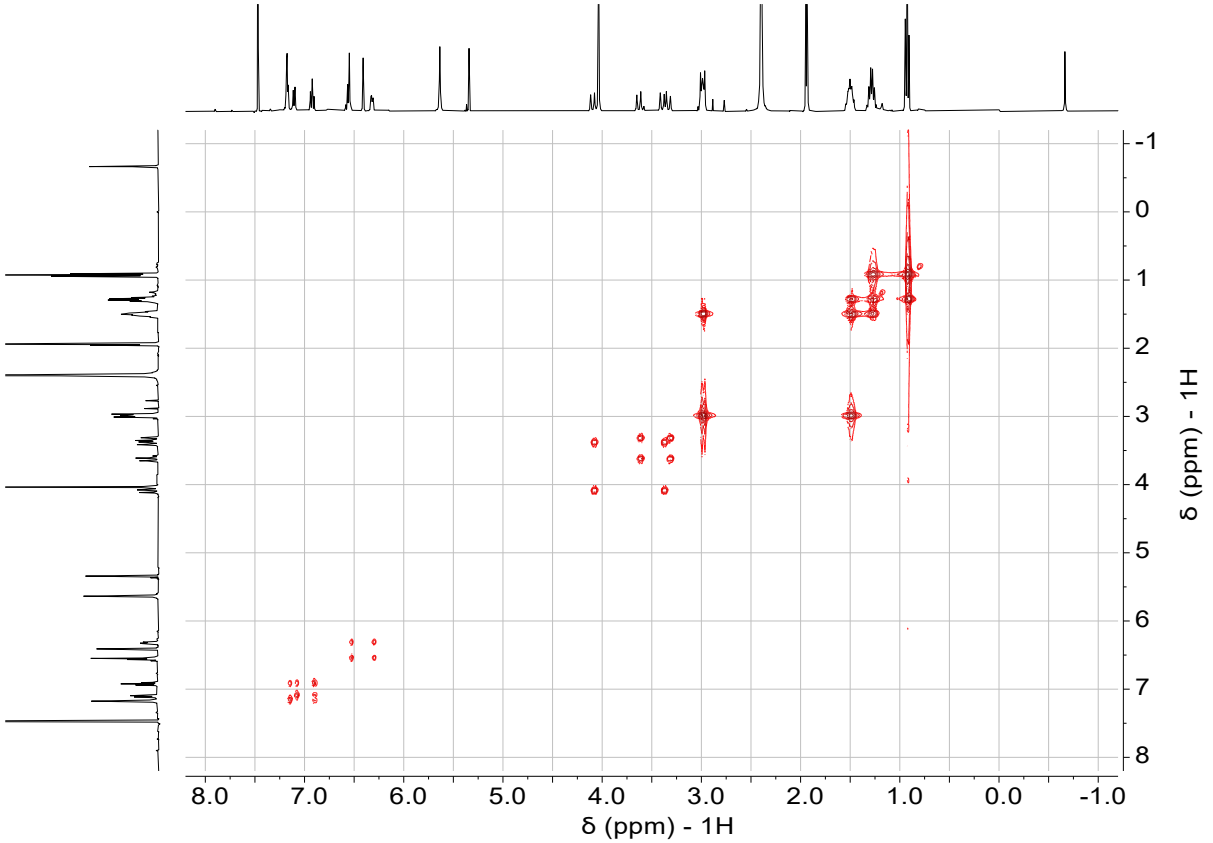

Figure SI47. COSY NMR (238K, 500 MHz) spectrum of [Zn(**3**)(G)]$(ClO_4)_2$ with 1 equiv. of TBAacetate in $CD_3CN/CDCl_3$ 1:1.

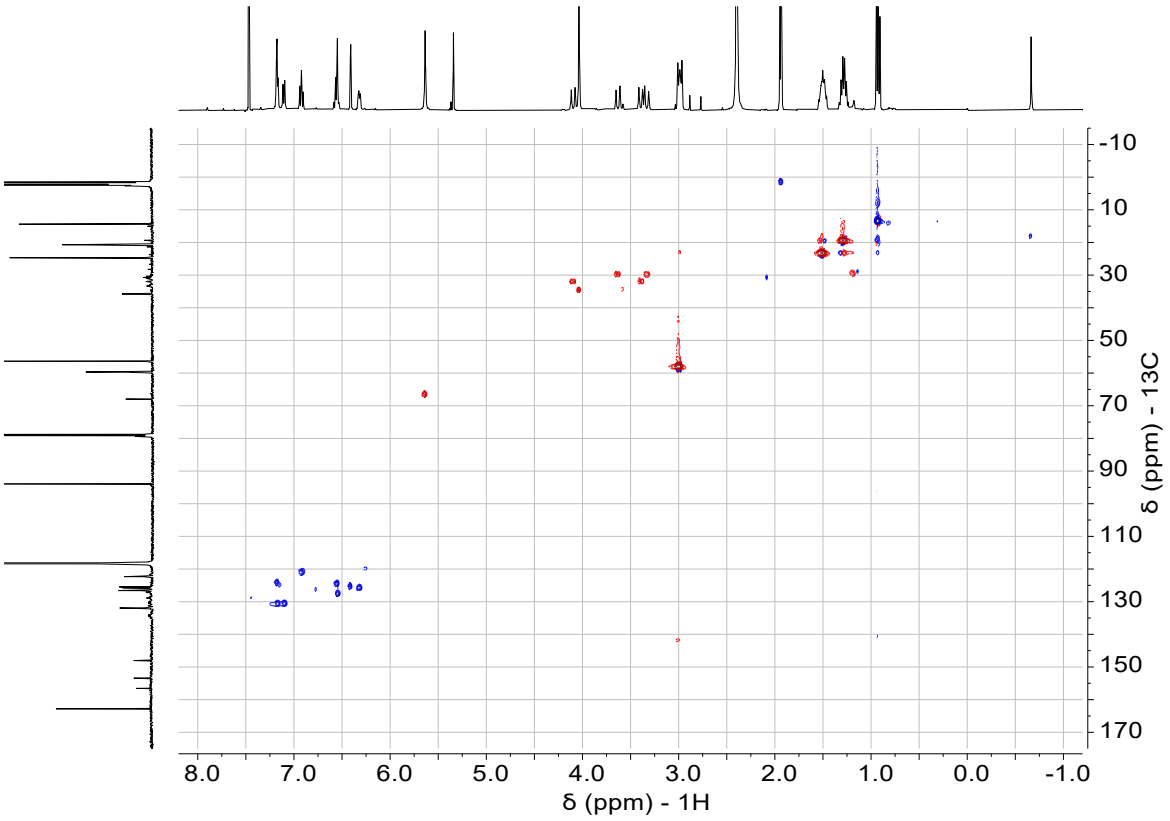

Figure SI48. HSQC NMR (238K, 400 MHz) spectrum of [Zn(**3**)(G)]$(ClO_4)_2$ with 1 equiv. of TBAacetate in $CD_3CN/CDCl_3$ 1:1.

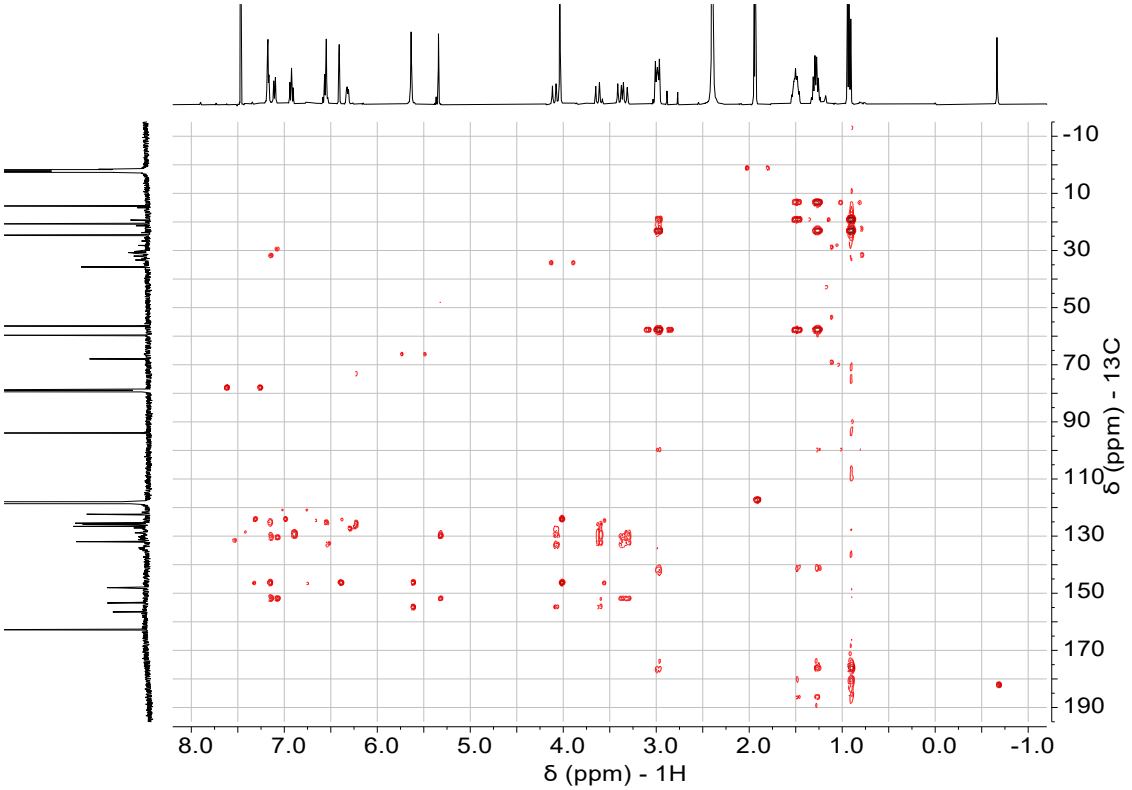

Figure SI49. HMBC NMR (238K, 400 MHz) spectrum of [Zn(**3**)(G)]$(ClO_4)_2$ with 1 equiv. of TBAacetate in $CD_3CN/CDCl_3$ 1:1. Additional note: The spectrum was not recorded at 238 K, as it would have required long acquisition time at low temperature.

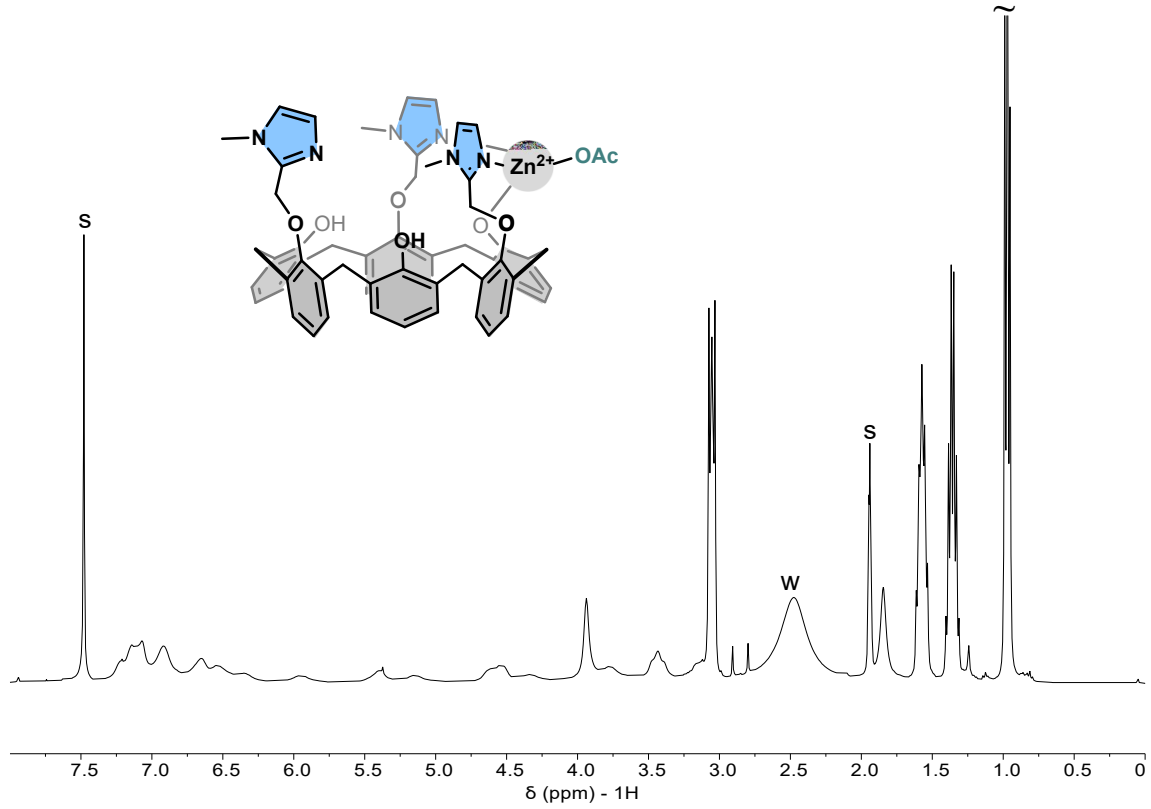

Figure SI50. ^1H NMR (298K, 400 MHz) spectrum of [Zn(**3**)(G)]$(ClO_4)_2$ with 2 equiv. of TBAacetate in $CD_3CN/CDCl_3$ 1:1. S: solvent, w: water.

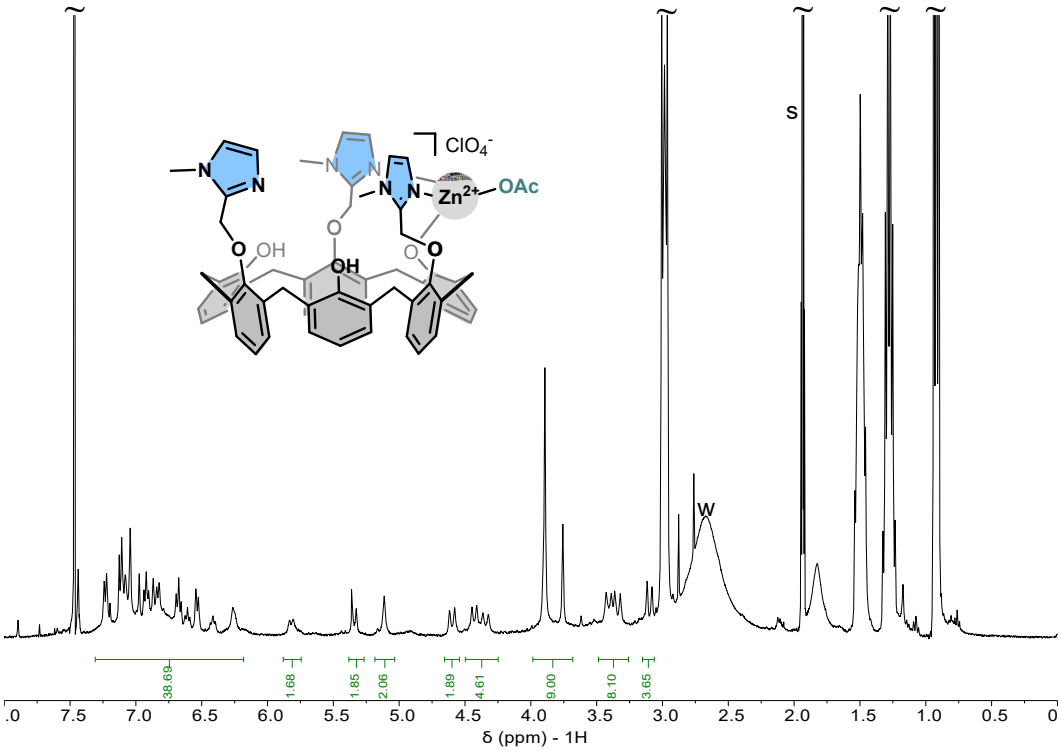

Figure SI51. ^{1}H NMR (238K, 400 MHz) spectrum of [Zn(**3**)(G)]$(ClO_4)_2$ with 2 equiv. of TBAacetate in $CD_3CN/CDCl_3$ 1:1. S: solvent, w: water. Additional note: The product was not completely soluble in the mixture at 238 K.

VIII. ^{1}H NMR analysis of [Zn(**2**)(G)](ClO$_4$)$_2$ in CD$_3$CN/CDCl$_3$ 1:1 with additions of an equimolar hexanoic acid/triethylamine solution.

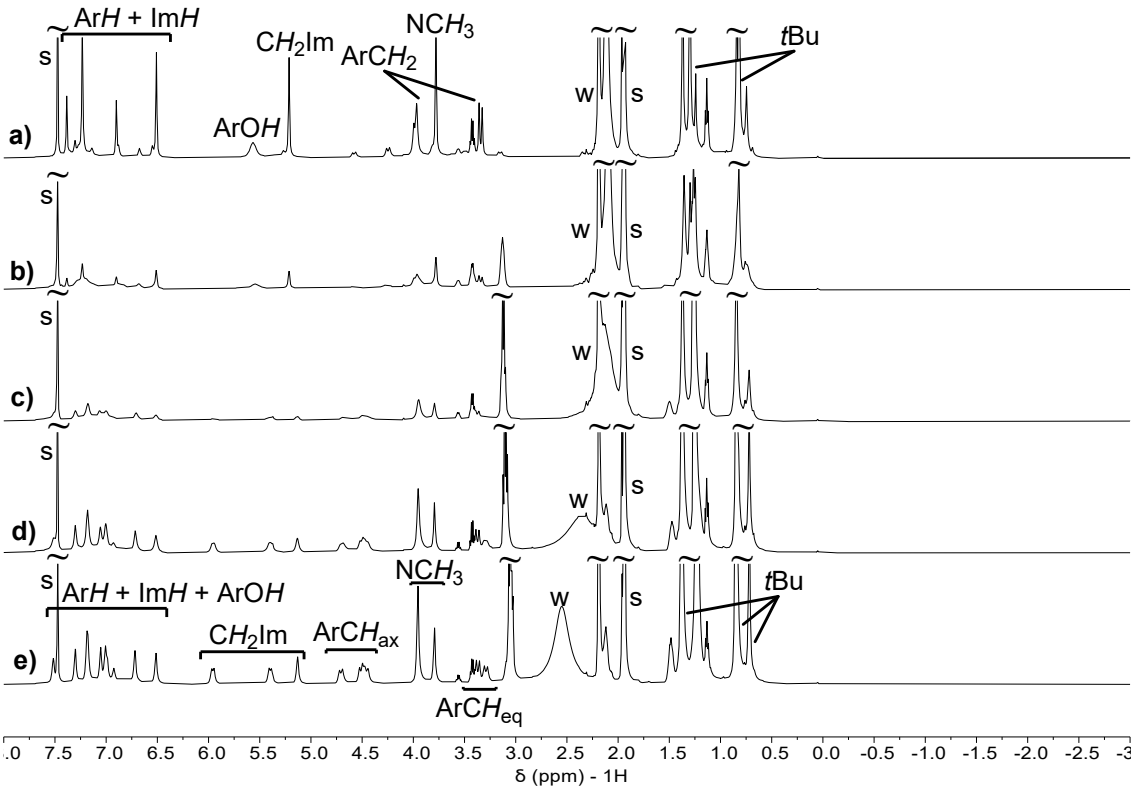

Figure SI52. ^{1}H NMR (298K, 500 MHz) titration showing the evolution of [Zn(**2**)(G)](ClO$_4$)$_2$ in CDCl$_3$/CD$_3$CN 1:1 by addition of a) before additions, b) 0.5 equiv. of hexanoic acid and triethylamine, c) 1 equiv. of hexanoic acid and triethylamine, d) 1,5 equiv. of hexanoic acid and triethylamine and e) 2 equiv. of hexanoic acid and triethylamine. S: solvent, w: water.

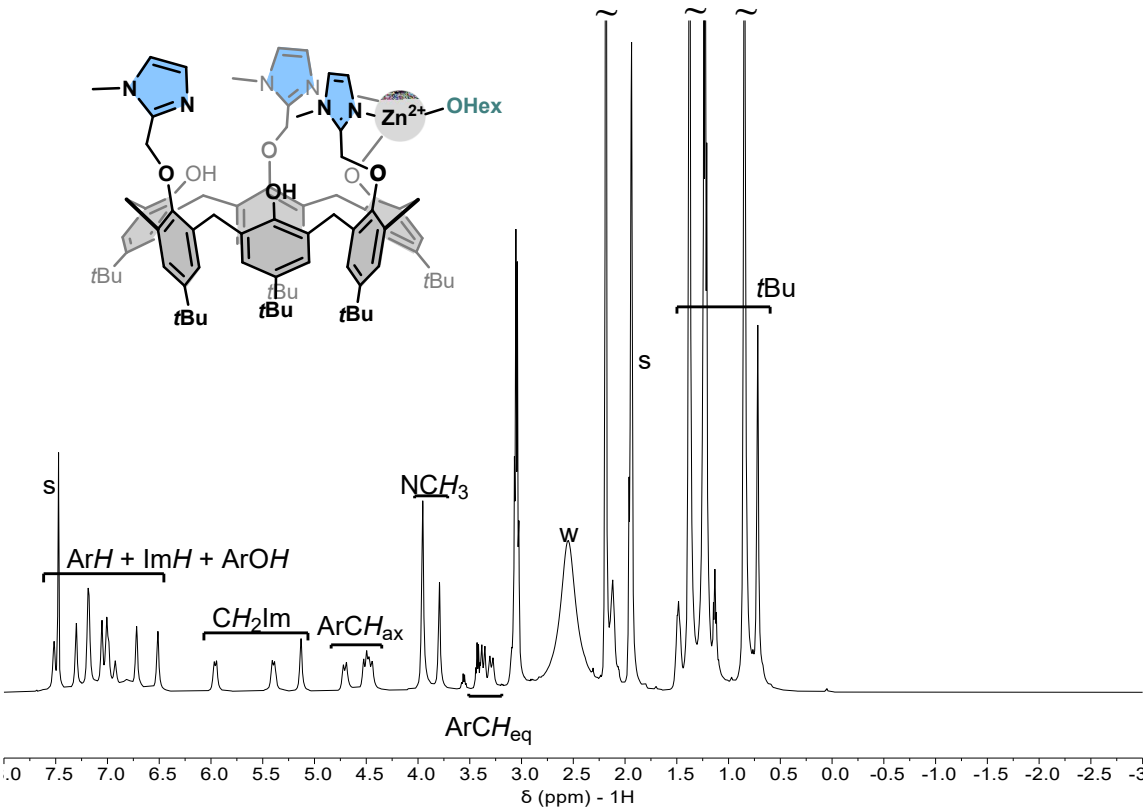

Figure SI53. ^{1}H NMR (298K, 500 MHz) spectrum of [Zn(**2**)(G)]$(ClO_4)_2$ with 2 equiv. of hexanoic acid and triethylamine in $CD_3CN/CDCl_3$ 1:1. S: solvent, w: water.

IX. ^{1}H NMR analysis of [Zn(**3**)(G)]$(ClO_4)_2$ in $CD_3CN/CDCl_3$ 1:1 with additions of an equimolar hexanoic acid/triethylamine solution.

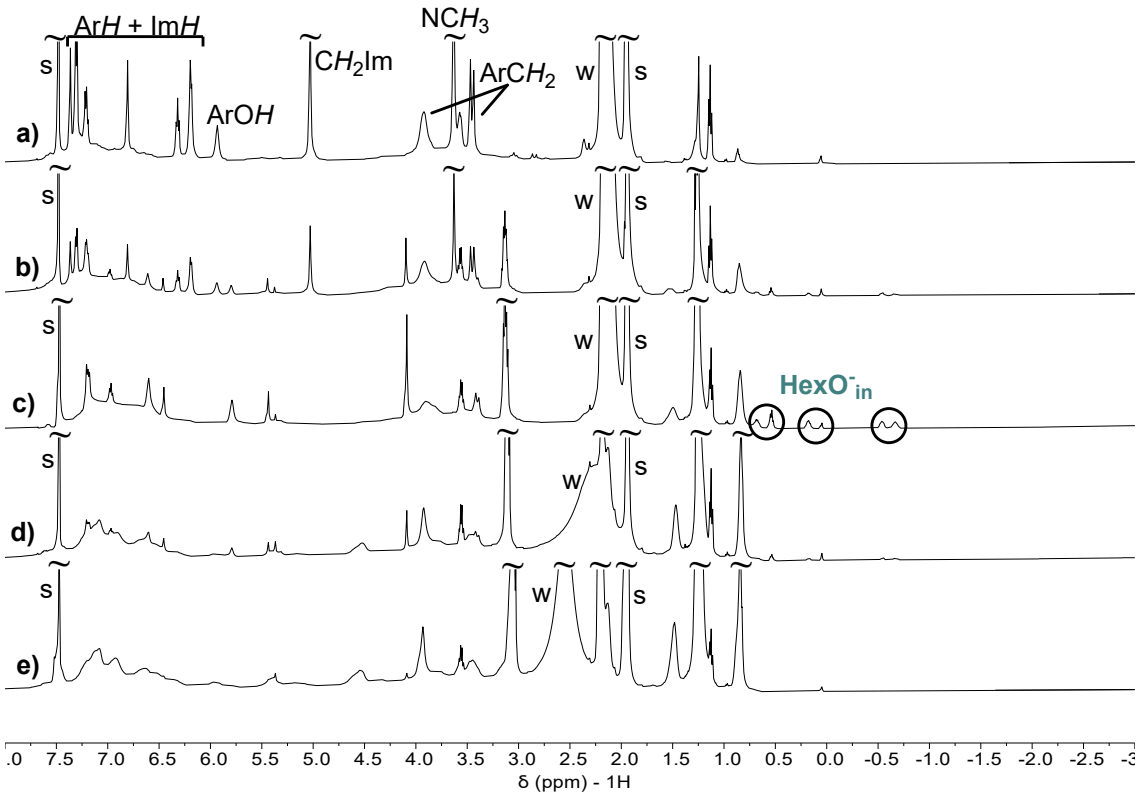

Figure SI54. ^{1}H NMR (298K, 500MHz) titration showing the evolution of [Zn(**3**)(G)]$(ClO_4)_2$ in $CDCl_3/CD_3CN$ 1:1 by addition of a) before additions, b) 0.5 equiv. of hexanoic acid and triethylamine, c) 1 equiv. of hexanoic acid and triethylamine, d) 1,5 equiv. of hexanoic acid and triethylamine and e) 2 equiv. of hexanoic acid and triethylamine. S: solvent, w: water.

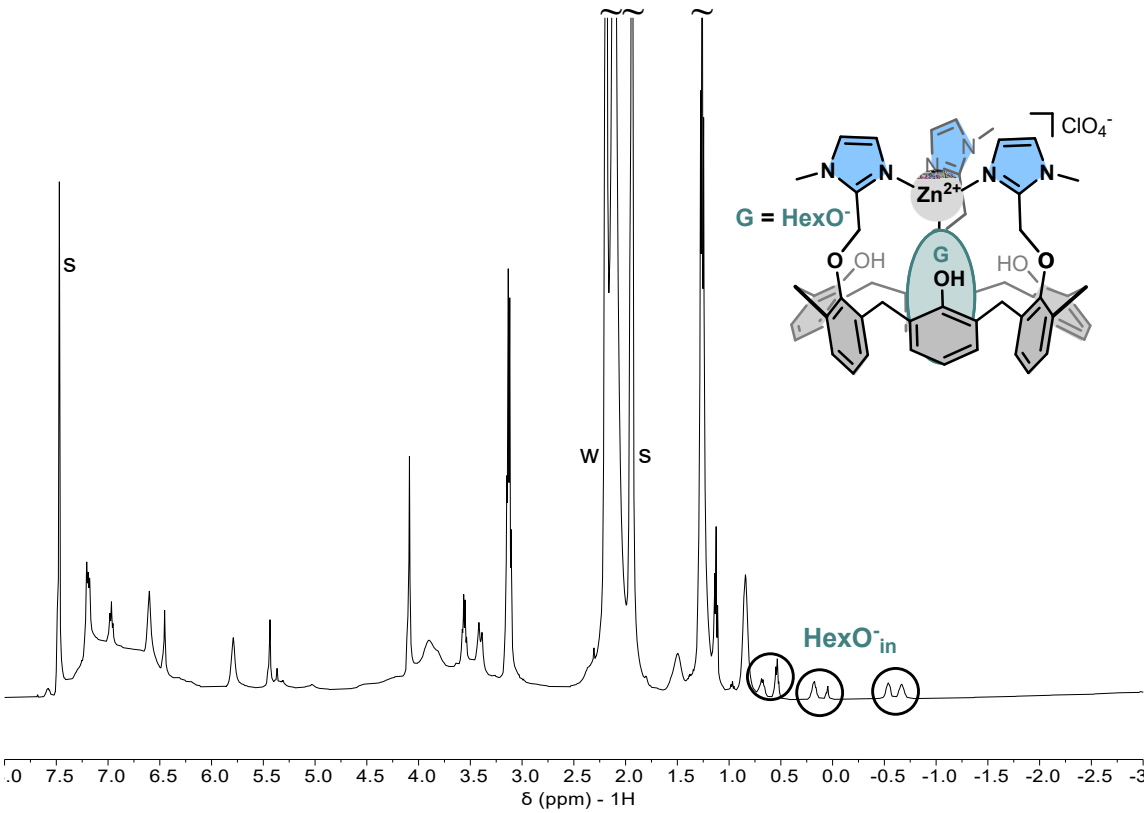

Figure SI55. ^{1}H NMR (298K, 500 MHz) spectrum of [Zn(**3**)(G)]$(ClO_4)_2$ with 1 equiv. of hexanoic acid and triethylamine in $CD_3CN/CDCl_3$ 1:1. S: solvent, w: water.

X. ^{1}H NMR analysis of [Zn(**2**)(G)](ClO$_4$)$_2$ in CD$_3$CN/CDCl$_3$ 1:1 with addition of tetrabutylammonium azide. ^{1}H NMR analysis of [Zn(**2**)(G)](TfO)$_2$ calix[6]arene in CD$_3$CN/CDCl$_3$ 1:1 with addition of tetrabutylammonium chloride.

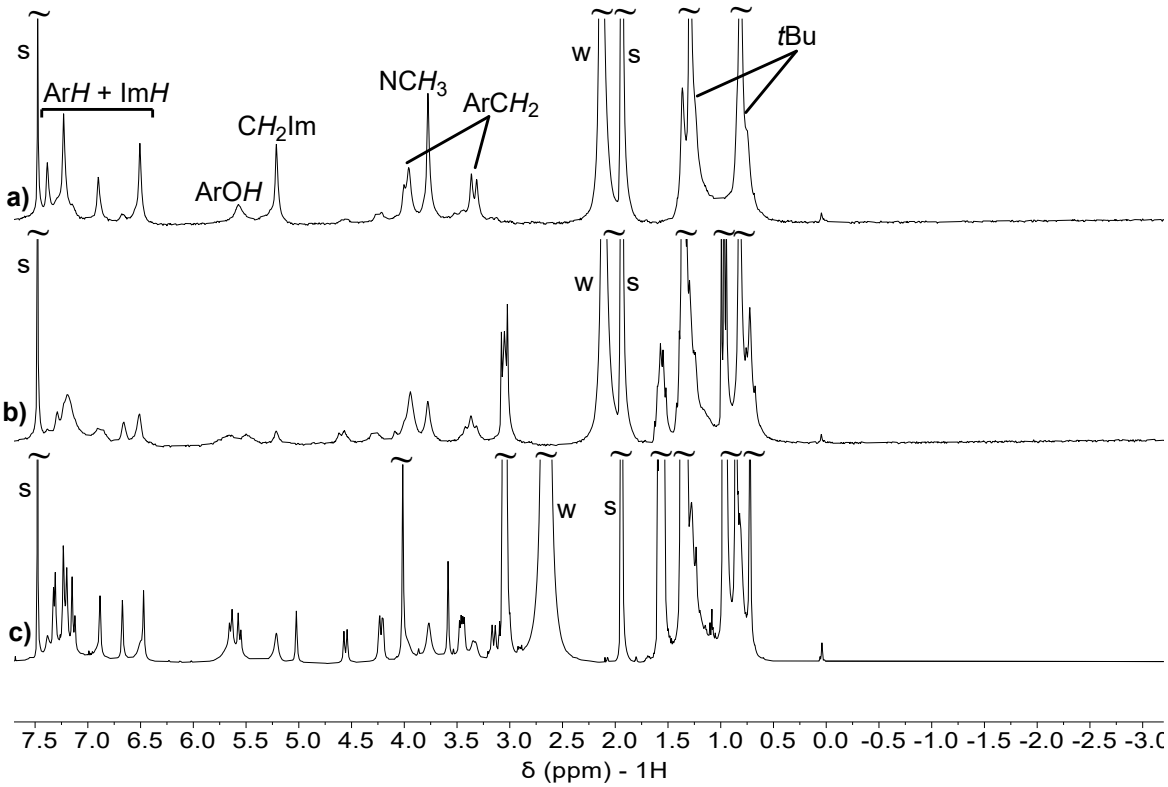

Figure SI56. ^{1}H NMR (298K, 500 MHz) titration showing the evolution of [Zn(**2**)(G)](ClO$_4$)$_2$ in CDCl$_3$/CD$_3$CN 1:1 by addition of a) before additions, b) 1 equiv. of TBAazide and c) 4 equiv. of TBAazide. S: solvent, w: water.

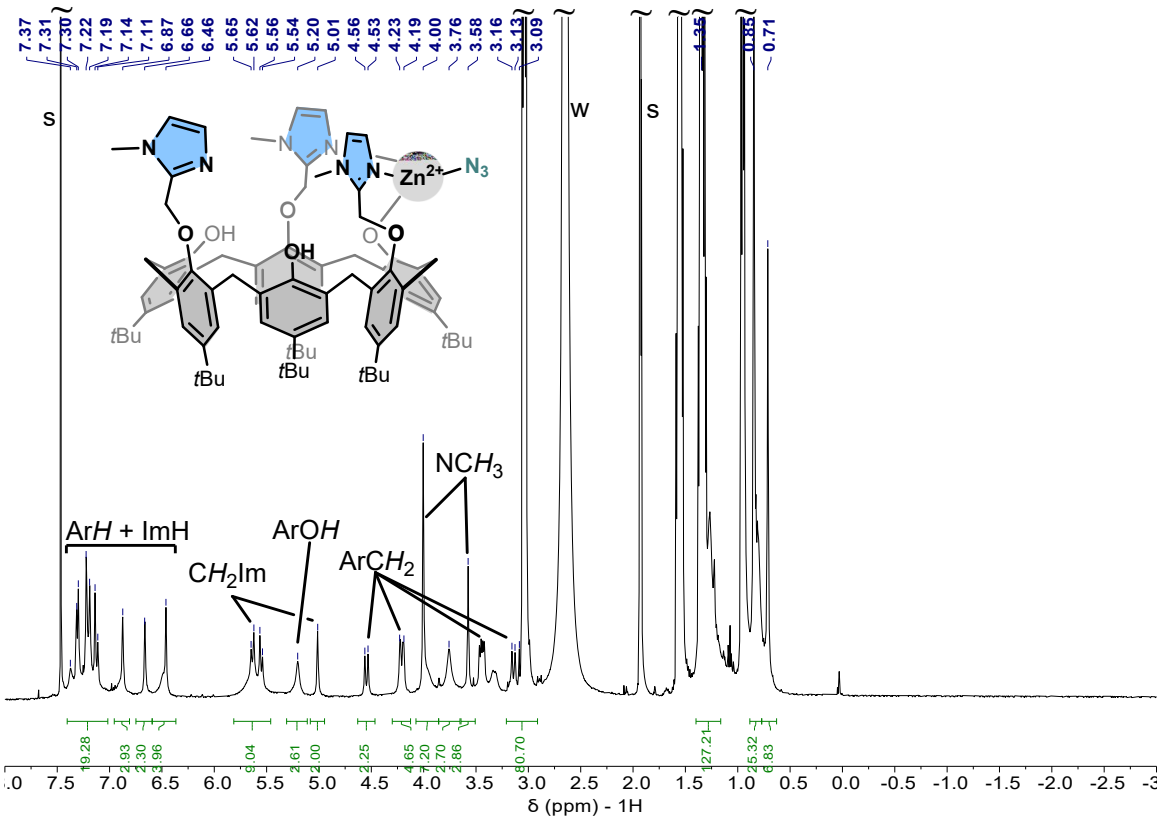

Figure SI57. ^{1}H NMR (298K, 500 MHz) spectrum of [Zn(**2**)(G)]$(ClO_4)_2$ with 4 equiv. of TBAazide in $CD_3CN/CDCl_3$ 1:1. S: solvent, w: water.

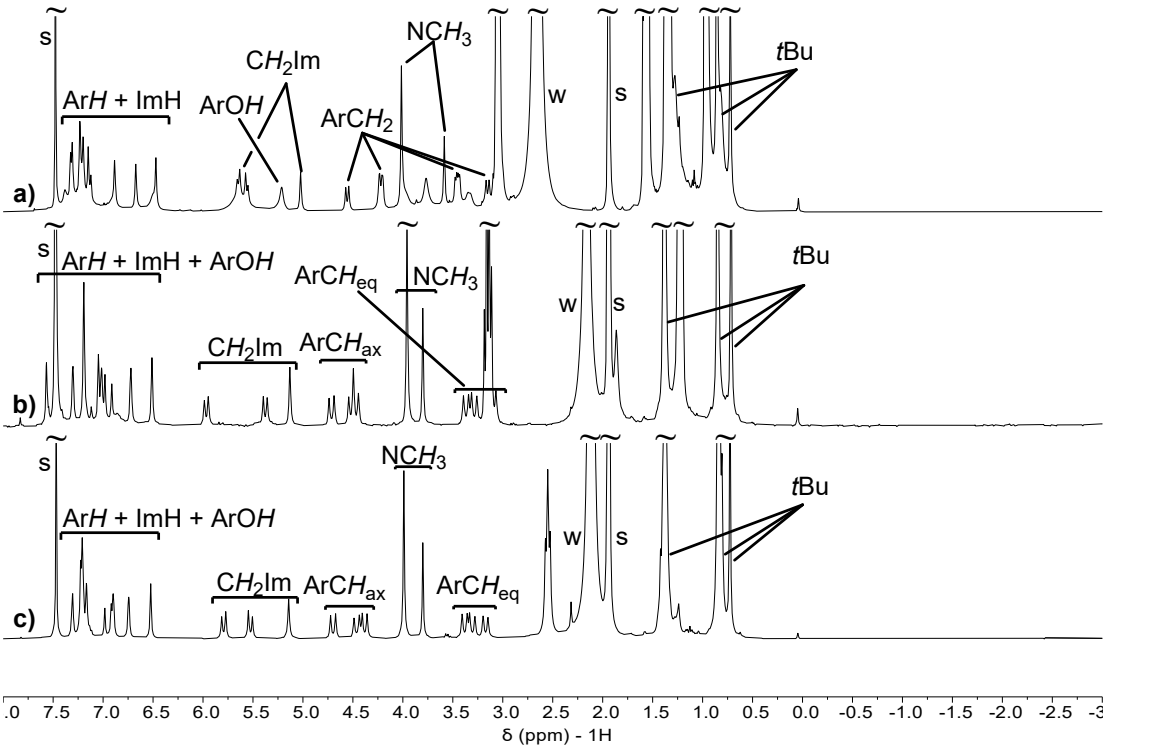

Figure SI58. ^{1}H NMR (298K, 500 MHz) spectrum comparison of [Zn(**2**)(G)]$(ClO_4)_2$ in $CD_3CN/CDCl_3$ 1:1 with a) 4 equiv. of TBAazide, b) 2.33 equiv. of TBAacetate and c) 8 equiv of propylamine. S: solvent, w: water.

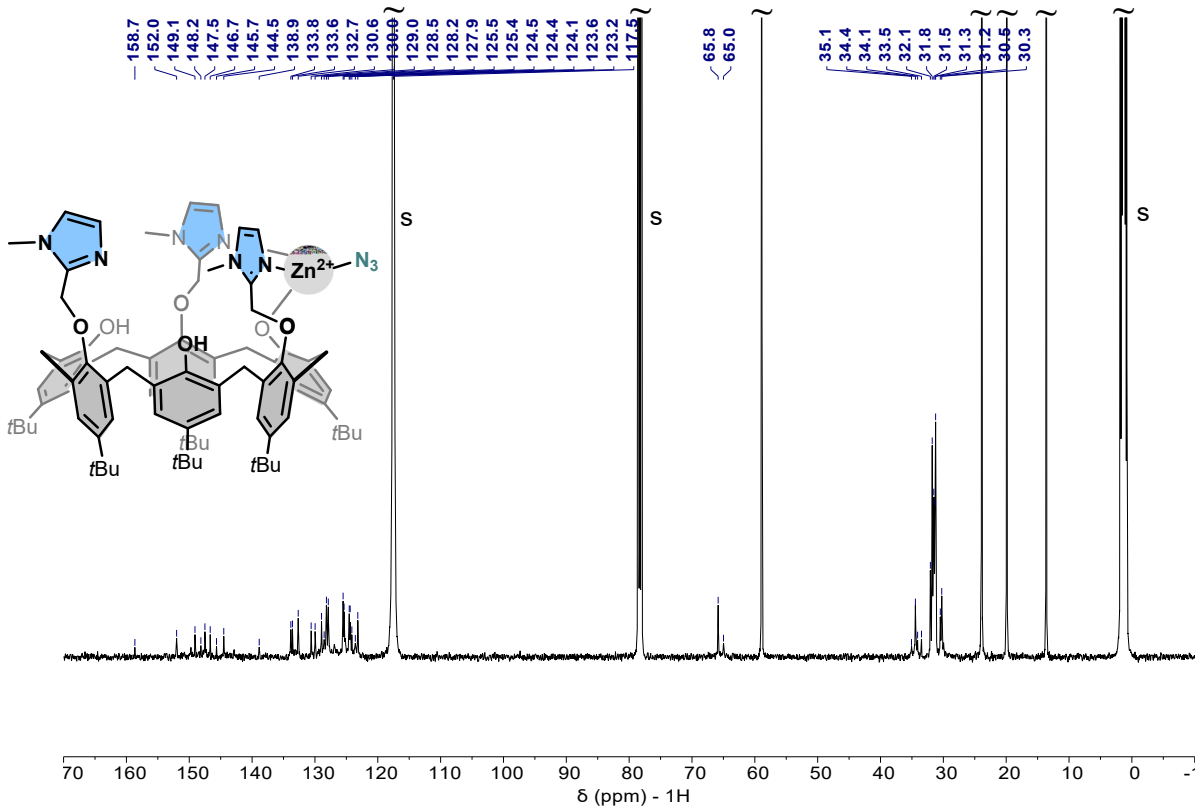

Figure SI59. ^{13}C NMR (298K, 126 MHz) spectrum of [Zn(**2**)(G)]$(ClO_4)_2$ with 4 equiv. of TBAazide in $CD_3CN/CDCl_3$ 1:1. S: solvent.

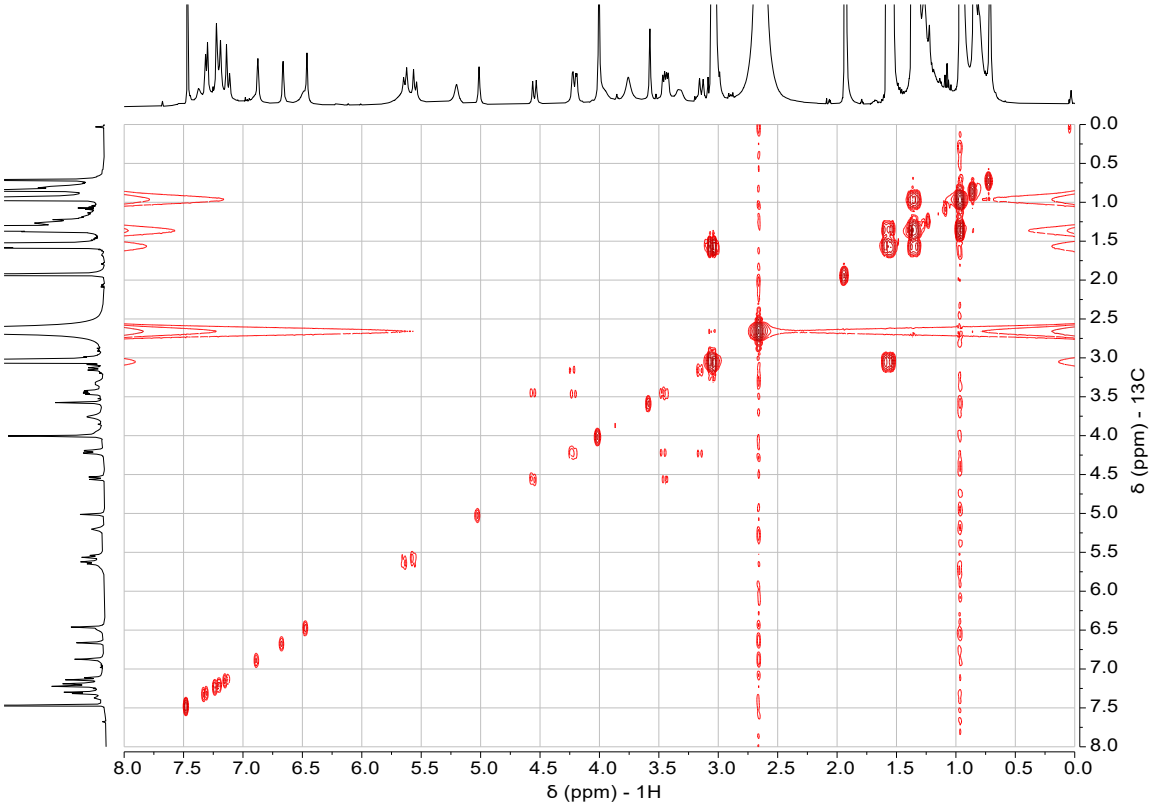

Figure SI60. COSY NMR (298K, 500 MHz) spectrum of [Zn(**2**)(G)]$(ClO_4)_2$ with 4 equiv. of TBAazide in $CD_3CN/CDCl_3$ 1:1.

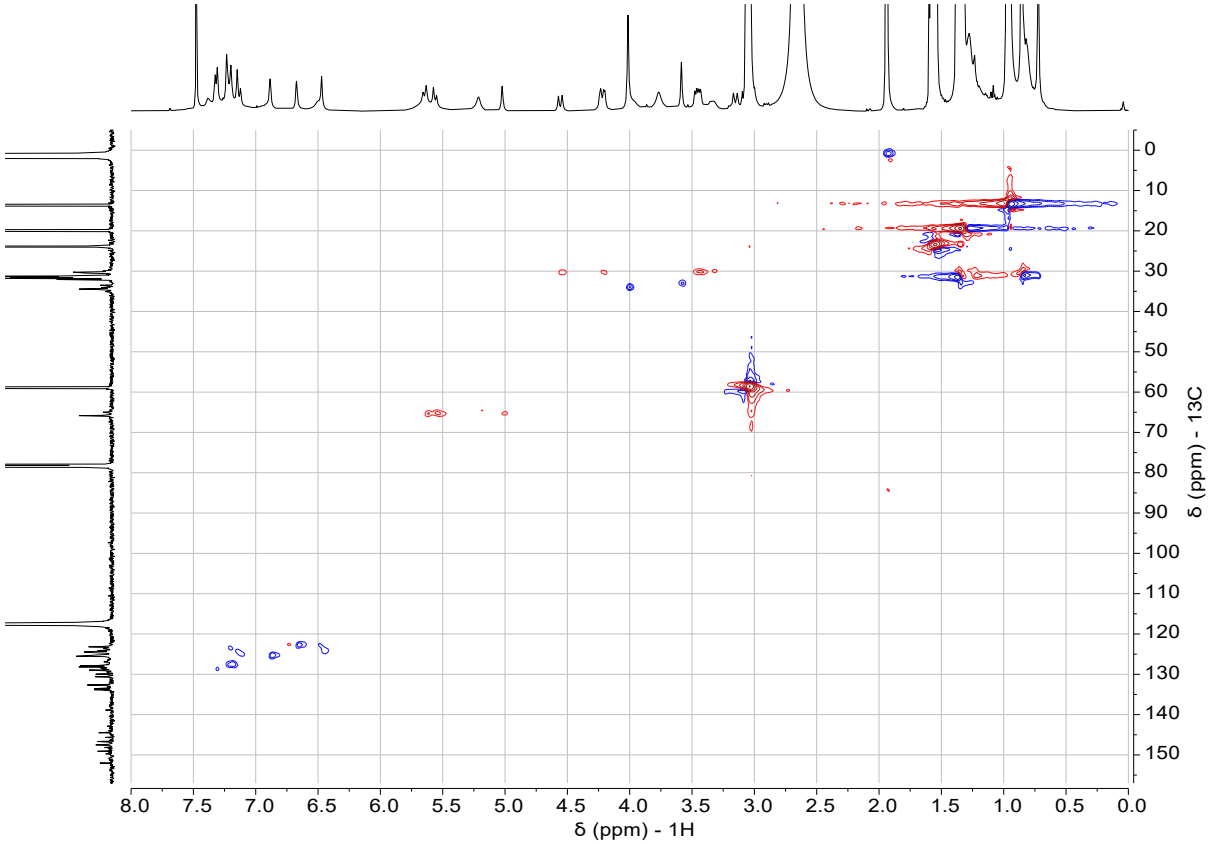

Figure SI61. HSQC NMR (298K, 500 MHz) spectrum of [Zn(**2**)(G)]$(ClO_4)_2$ with 4 equiv. of TBAazide in $CD_3CN/CDCl_3$ 1:1.

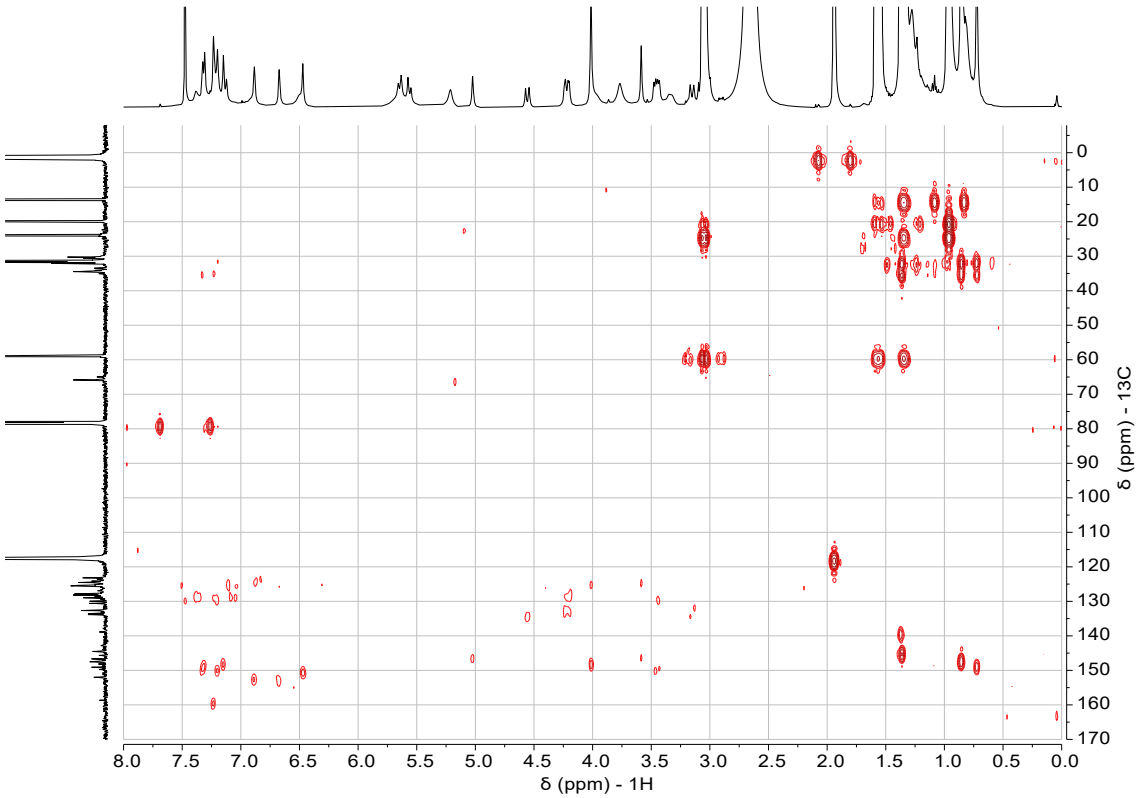

Figure SI62. HMBC NMR (298K, 400MHz) spectrum of [Zn(**2**)(G)]$(ClO_4)_2$ with 4 equiv. of TBAazide in $CD_3CN/CDCl_3$ 1:1.

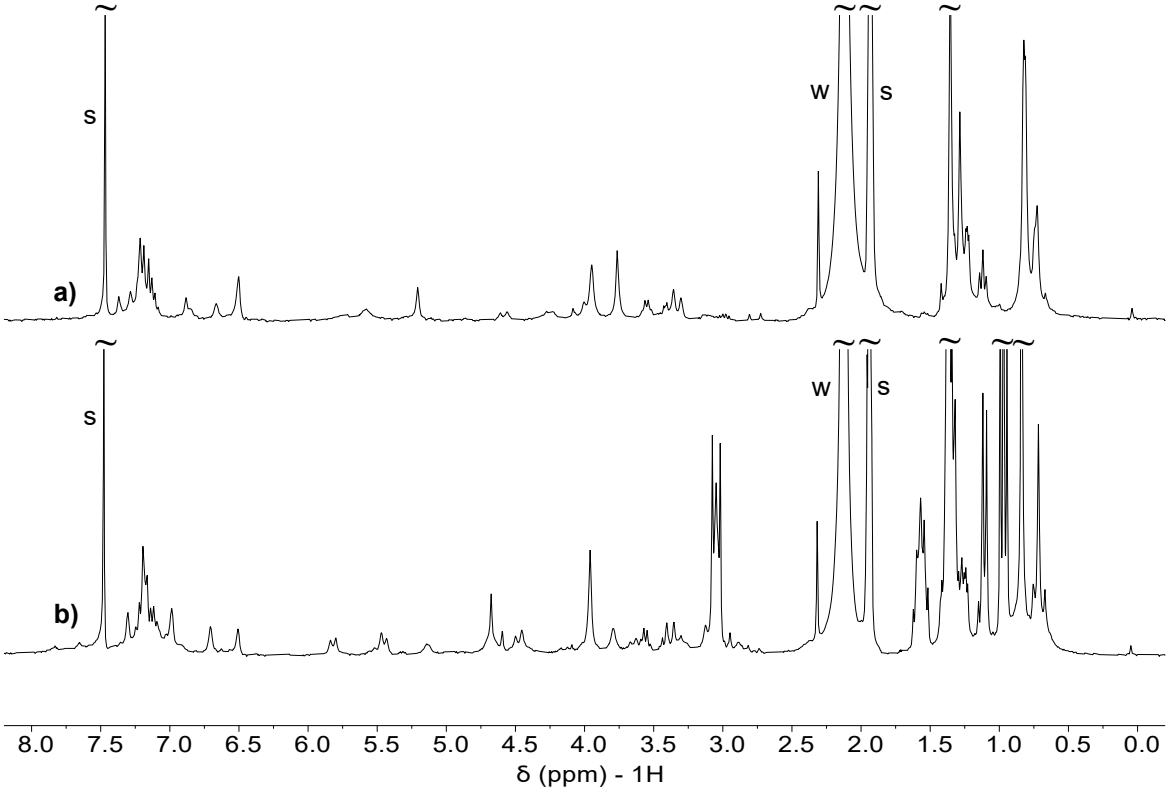

Figure SI63. ^{1}H NMR (298K, 300 MHz) titration showing the evolution of [Zn(**2**)(G)](OTf)$_2$ in $CDCl_3/CD_3CN$ 1:1 by addition of a) before additions, b) 1 equiv. of TBACl. S: solvent, w: water.

XI. ^{1}H NMR analysis of [Zn(**2**)(G)](ClO$_4$)$_2$ in CDCl$_3$ with incremental additions of a sodium acetate in D$_2$O solution.

The ability of [Zn(**2**)(G)](ClO$_4$)$_2$ to extract acetate from an aqueous phase was evaluated. A biphasic extraction experiment was conducted by gradually adding a D$_2$O solution containing sodium acetate (9.5 mM) to a CDCl$_3$ solution of [Zn(**2**)(G)](ClO$_4$)$_2$ (2.4 mM). After vigorous mixing, ^{1}H NMR spectra of the organic phase were recorded to monitor the extraction (Figure SI64). Due to its limited solubility in CDCl$_3$ and probably the lack of a suitable guest, the receptor exhibited a poorly defined spectrum under these conditions. Nevertheless, up to equimolar acetate-to-receptor ratios, the typical high-field resonance at –0.80 ppm was observed, confirming successful extraction of acetate into the organic phase. At higher acetate concentrations in the aqueous phase, the receptor predominantly existed in its deprotonated form, consistent with the behaviour observed in homogeneous media.

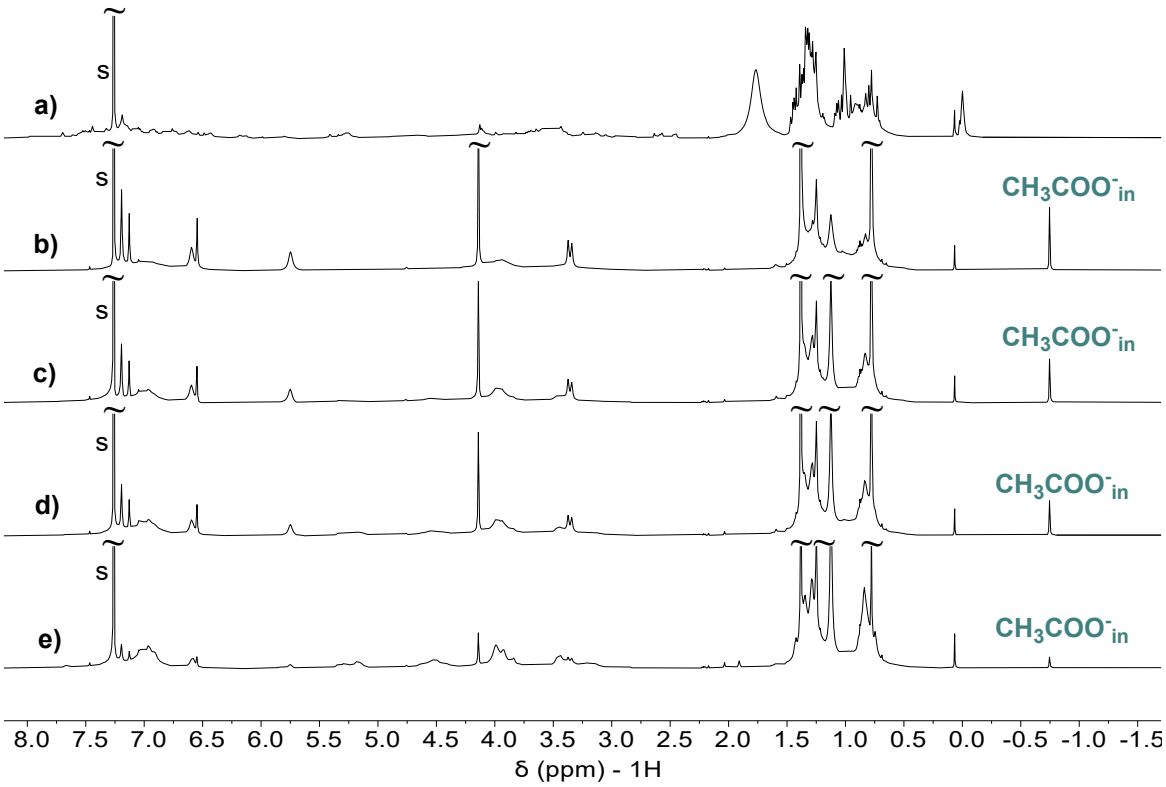

Figure SI64. ^{1}H NMR (298K, 500MHz) spectrum of the titration of [Zn(**2**)(G)](ClO$_4$)$_2$ in CDCl$_3$ 1:1 with a) before additions, b) 0.5 equiv. of sodium acetate in D$_2$O, c) 1 equiv. of sodium acetate in D$_2$O, d) 2 equiv. of sodium acetate in D$_2$O and e) 4 equiv. of sodium acetate in D$_2$O. S: solvent. Additional note: [Zn(**2**)(G)](ClO$_4$)$_2$ was not completely soluble during the experiment, equivalents of sodium acetate were calculated based on the initial amount of [Zn(**2**)(G)](ClO$_4$)$_2$ added to the NMR tube.

XII. Cristallographic data.

Crystal Structure Analysis of [Zn(3)(CH_3CN)](ClO_4)$_2$: X-ray-quality crystals were grown by slow diffusion of tert-butyl methyl ether into a 1:1 acetonitrile/chloroform solution of the complex.

Crystal Structure Analysis of [Zn(3)(CH_3CN)](ClO_4)$_2$ in presence of propylamine: X-ray-quality crystals were grown by slow diffusion of diethyl ether into a 1:1 acetonitrile/chloroform solution of the complex and 4 equiv. of propylamine.

Crystal Structure Analysis of [Zn(2)(OAc)](ClO_4): X-ray-quality crystals were grown by slow diffusion of diethyl ether into a 1:1 acetonitrile/chloroform solution of the complex and 1 equiv. of tetrabutylammonium acetate.

X-ray diffraction data. Crystal data, data collection and refinement parameters are summarized in Table SI1. For [Zn(**3**)(CH_3CN)](ClO_4)$_2$ (CCDC 2442674) and [Zn(**2**)(OAc)](ClO_4) (CCDC 2442673), data reduction and cell refinement were carried out using the CRYSALIS PRO software [1], and standard multi-scan absorption correction was applied. For [Zn(**3**)(CH_3CN)](ClO_4)$_2$ in presence of propylamine (CCDC 2442675), data collection was performed at the Elettra synchrotron beam line XRD2, and controlled by MXCuBE,[2] while data reduction and cell refinement were conducted by XDS.[3] Structures were solved by direct methods with SHELXT [4], and refined by a full matrix least-squares refinement based on F^2, with SHELXL [5], included into the OLEX2 [6] interface. Hydrogen atoms were included in their geometrically calculated positions and refined according to the riding model.

Table SI1. Crystallographic data

Structure	$[Zn(\mathbf{3})(CH_3CN)](ClO_4)_2$ in presence of propylamine (CCDC 2442675)	$[Zn(\mathbf{3})(CH_3CN)](ClO_4)_2$ (CCDC 2442674)	$[Zn(\mathbf{2})(OAc)](ClO_4)$ (CCDC 2442673)
Brutto form.	$C_{236}H_{224}Cl_4\ N_{28}O_{40}Zn_4$	$C_{63}H_{63}Cl_2N_9O_{14}Zn$	$C_{182}H_{246}Cl_3N_{13}O_{28}Zn_2$
M_r (gmol^{-1})	4495.70	1306.56	3294.59
Moiety form.	$C_{57}H_{53}N_6Zn$ x CH_3CN, ClO_4	$C_{57}H_{54}N_6Zn$ x CH_3CN, $2CH_3CN$, $2ClO_4$	$2(C_{81}H_{102}N_6O_6Zn$ x $CH_3COO)$, $C_{16}H_{36}N$, $3(ClO_4)$
Crystal color/hab	Colourless prism	Colourless prism	Colourless needle
Cryst. (mm)	0.10 x 0.05 x 0.02	0.20 x 0.17 x 0.15	0.08 x 0.03 x 0.02
F (000)	9375	1363	2871
μ (mm^{-1})	0.325	1.843	0.794
Space group (No.)	*Ccce* (68)	*P*-1 (2)	*P*-1 (2)
a (Å)	26.685 (5)	13.22765 (11)	16.4168 (7)
b (Å)	39.811 (8)	14.15549 (10)	24.6211 (9)
c (Å)	24.924 (5)	17.82870 (14)	25.3326 (6)
α (°)	90.	85.7263 (6)	98.772 (2)
β (°)	90.	81.2491 (7)	93.648 (3)
γ (°)	90.	86.7523 (6)	97.939 (3)
V (Å^3)	26478 (9)	3286.80 (4)	9985.1 (6)
Z (Z')	4	2	2
Instrument	Elettra synchrotron	XtaLAB Synergy	XtaLAB Synergy
Radiation (Å)	0.62	Cu$K\alpha$, 1.54184	Cu$K\alpha$, 1.54184
Temperature (K)	100	120	150
R_{int}	0.1183	0.0378	0.0609
R_σ	0.0517	0.0342	0.1120
θ_{max} (°)	20.346	79.85	53.740
Unique	9757	14021	16875
Obs. [$I>2\sigma(I)$]	7141	12432	9161
Parameters	556	812	2137
R_1 [$I>2\sigma(I)$]	0.103	0.054	0.078
wR_2, all	0.358	0.144	0.232
S	1.50	1.03	1.00
ρ_{max}, ρ_{min} (eÅ^{-3})	1.25; -0.49	1.79; -1.49	0.75; -0.47
Solvent mask	Olex2[6]	Olex2[6]	Olex2[6]

XIII. References.

[1] CrysAlis CCD, Oxford Diffraction Ltd., Version 1.171.32.29 (release 10-02008 CrysAlis171.NET).

[2] U. Mueller, M. Thunnissen, J. Nan, M. Eguiraun, F. Bolmsten, A. Milàn-Otero, M. Guilarro, M. Oscarsson, D. de Santis, and G. Leonard, *Synchrotron Radiation News,* 2017, **30**, 22.

[3] W. Kabsch, *Acta Cryst. D,* 2010, **66**, 125.

[4] G. M. Sheldrick, *Acta Cryst. A,* 2015, **71**, 3.

[5] G. M. Sheldrick, *Acta Cryst. C,* 2015, **71**, 3.

[6] O. V. Dolomanov, L. J. Bourhis, R. J. Gildea, J. A. K. Howard, and H. Puschmann, *J. Appl. Cryst*., 2009, **42**, 339.